Bioorganic Chemistry 110 (2021) 104793

Contents lists available at ScienceDirect

Bioorganic Chemistry

journal homepage: www.elsevier.com/locate/bioorg

Structure-activity relationships and antiproliferative effects of 1,2,3,4-4*H*-quinoxaline derivatives as tubulin polymerization inhibitors

Tingting Liang [a], Xiaomin Zhou [a], Lu Lu [a], Haiyang Dong [a], Yanan Zhang [a], Yungen Xu [b], Jianguo Qi [a,*], Yahong Zhang [a,*], Jianhong Wang [a,*]

[a] Key Laboratory of Natural Medicine and Immune-Engineering of Henan Province, Henan University Jinming Campus, Kaifeng 475004, Henan, China
[b] Jiangsu Key Laboratory of Drug Design and Optimization, Department of Medicinal Chemistry, China Pharmaceutical University, Nanjing 211198, China

ARTICLE INFO

Keywords:
Colchicine binding site
Inhibitors
Tetrahydro-quinoxaline derivatives
Antitumor activities

ABSTRACT

Colchicine binding site inhibitors (CBSIs) hold great potential for the treatment of various tumors and they can overcome multidrug resistance which the existing tubulin inhibitors such as paclitaxel and vinorelbine are faced with. Herein, we report the design, synthesis and biological evaluation of a series of tetrahydro-quinoxaline derivatives as colchicine binding site inhibitors. All the synthesized compounds were evaluated for their *in vitro* antiproliferative activities against HT-29 and Hela cancer cell lines, and most of the target compounds demonstrated moderate to strong activities towards two tumor cell lines. In addition, the structure-activity relationships of these derivatives were also discussed. Among them, compounds **11a** and **11b** showed the most potent activities. Moreover, compound **11a** inhibited the tubulin polymerization in both cell-free and cellular assays. Further profiling of compound **11a** revealed that it arrested cell cycle in G2/M and induced cell apoptosis in a dose-dependent manner. Furthermore, molecular docking study proved that compound **11a** acted on the colchicine binding site. Therefore, **11a** is a promising candidate for the discovery of colchicine binding site inhibitors.

1. Introduction

Microtubules are important components of the eukaryotic cytoskeleton, which are composed of α-tubulin and β-tubulin subunits in a head-to-tail arrangement [1–4]. And the dynamic equilibrium process of polymerization / depolymerization is closely related to maintain cell architecture [3,5,6] and regulate mitosis by forming spindle and separating chromosomes [7–10]. Additionally, microtubules are also involved in intracellular transport, organelle positioning, cell motility, signaling control and so on [11,12]. Therefore, microtubules have been one of the most attractive targets in the treatment of cancer, and disrupting microtubule dynamics is an important strategy to develop novel microtubule-targeting agents (MTAs) [13–15].Fig. 1

Based on the mechanisms of action, MTAs are generally divided into two major classes: microtubule stabilizing agents and microtubule destabilizing agents. According to their different binding sites, the microtubule stabilizing agents act on the taxane and laulimalid binding sites, while the microtubule destabilizing agents act on the vinca alkaloids, colchicine, maytansine and pironetin binding sites [16,17]. Over the past decades, MTAs such as paclitaxel and vinca alkaloids have been approved by the FDA for the treatment of tumors which show great success. However, their therapeutic applications are usually limited by multidrug resistance.

Colchicine binding site inhibitors (CBSIs) can not only perturb mitosis and induce cell death, but also disrupt tumor blood vessels to inhibit nutrients and oxygen delivery to the tumor tissues, acting as vascular disrupting agents [18,19]. Moreover, accumulating evidence suggests that CBSIs have been considered as candidates to overcome multidrug resistance (MDR) for that CBSIs are not the substrates of the MDR efflux pump [20,21]. Therefore, CBSIs gain more and more attentions from medicinal chemists as new generation agents in cancer chemotherapy. Colchicine, the first identified CBSI, suffers from high toxicity and narrow therapeutic index, which limit its clinical use [22]. Combretastatins including CA-1, CA-2 and CA-4 show strong tubulin polymerization inhibitory activities, but their clinical applications are limited by low bioavailability and isomerization which generates the less active *trans* isomer [23]. To address their shortcomings, many novel CBSIs have been synthesized [11,16,24–26]. For example, Priego and

* Corresponding authors.
E-mail addresses: qijianguo@henu.edu.cn (J. Qi), zhangyahong_131@163.com (Y. Zhang), jhworg@126.com (J. Wang).

https://doi.org/10.1016/j.bioorg.2021.104793
Received 17 November 2020; Received in revised form 28 February 2021; Accepted 1 March 2021
Available online 5 March 2021

co-workers demonstrated the α-methyl chalcone TUB091 as potent tubulin polymerization inhibitor with IC_{50} value being 1–10 nM against cancer and endothelial cells [27]. Subsequently, based on conformational mimetics of TUB091, they constructed 1,2,3,4-tetrahydronaphthalen-2-yl aryl ketone (**1**) which exhibited potent antiproliferative activity and arrested cell cycle in G2/M phase in 2018. Particularly, **1** showed equivalent colchicine site binding ability with combretastatin A4 [28]. Recently, Bortolozzi *et al.* reported a 2-amino-3-(3′,4′,5′-trimethoxybenzoyl)-benzo[*b*]furan scaffold (**2**) as remarkable antiproliferative agent with IC_{50} being 5 pM against tumor cells, and they revealed that the powerful antiproliferative activity was attributed to the tubulin polymerization inhibition caused by binding to the colchicine site [29]. To date, several CBSIs have been in the clinical trials for treating various cancers. However, no CBSIs have been launched for the clinical use [26,30]. Therefore, it is imperative to develop new microtubule-targeting agents with novel structures that bind to the colchicine binding site.

Previously, our group have reported 3,4-dihydroquinixalin-2(1*H*)-one and 1,4-dihydroquinoxaline-2,3-dione derivatives as colchicine binding site inhibitors [31,32]. Based on the previous studies, we replaced the above scaffolds with 1,2,3,4-tetrahydro-quinoxaline scaffold to find novel compounds with high antitumor activity and complement the prior structural optimizations. Herein, we reported the design, synthesis and biological evaluation of 1,2,3,4-tetrahydroquinoxaline derivatives. All target compounds were evaluated for their antiproliferative activities against Hela and HT-29 cancer cell lines. The most active derivative was assessed for its tubulin depolymerization activity, the effects on cell cycle and cell death. The binding modes of 1,2,3,4-tetrahydroquinoxaline derivatives with tubulin through the molecular docking study were also predicted.

2. Results and discussions

2.1. Chemistry

The target compounds were summarized as depicted in Scheme 1. Commercially available material anilines **3b**–**3d** were mono-substituted with corresponding halides to give intermediates **4a**–**4j**, which were further reduced by hydrogenation with Pd/C to synthesize amines **5b**–**5k**. Intermediate **5a** was synthesized by nucleophilic substitution of 1,2-diaminobenzene **3a** with corresponding halide. Then condensation of intermediates **5a**–**5k** with dimethyl oxalate gave intermediates **6a**–**6k**, followed by reduction of intermediates **6a**–**6k** to yield the target compounds **7a**–**7k**. Compound **7d** was protected with $(Boc)_2O$ to obtain the intermediate **8** and followed by debenzylation to provide intermediate **9**. Condensation of **9** with acyl chlorides produced intermediates **10a**–**10l**, which underwent deprotection to furnish the final compounds **11a**–**11l**.

2.2. Biological evaluations

2.2.1. In vitro antiproliferative activities

All synthetic target compounds were evaluated for their antiproliferative activities against Hela and HT-29 cancer cell lines using MTT assay, compounds **12**, **13**, colchicine and CA-4 were chosen as positive controls. As demonstrated in Table 1, most of the target compounds showed antiproliferative activities against cancer cells with IC_{50} values under 15 μM.

Preliminary structure-activity relationships analysis was focused on the following three directions: substituents on the tetrahydroquinoxaline ring (R^1), the aromatic ring R^2 and the linker. When the linker was

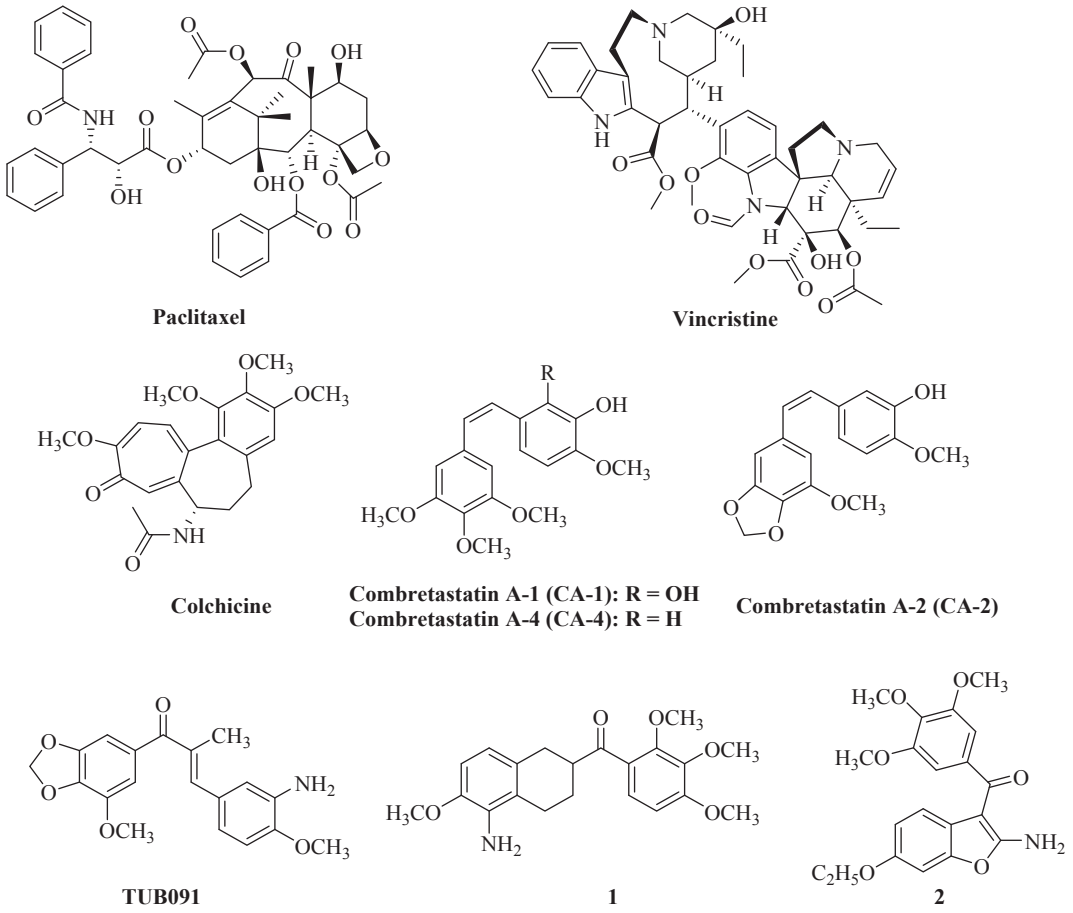

Fig. 1. Representative microtubule-targeting agents.

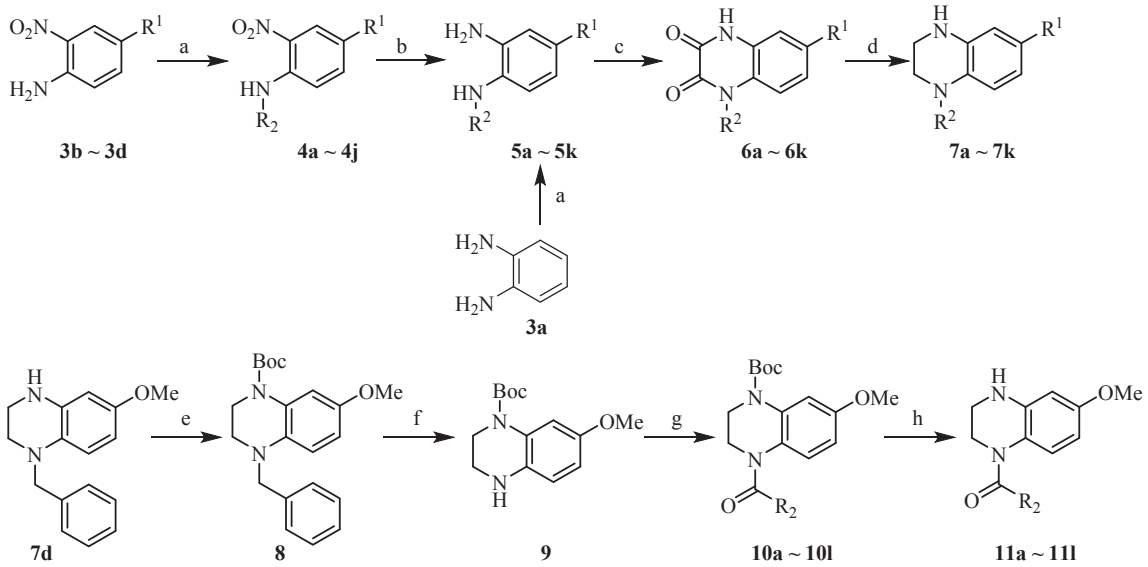

Scheme 1. Reagents and conditions: (a) corresponding halides, KI, K_2CO_3, MeCN, 70 °C, 6 h; (b) 10% Pd/C, H_2, MeOH, rt, 2 h; (c) dimethyl oxalate, 70 °C, 5 h; (d) BH_3-THF, anhydrous THF, 0 °C, 30 min then rt, 12 h; (e) $(Boc)_2O$, TEA, DCM, 40 °C, 15 h; (f) 10% Pd/C, H_2, MeOH, rt, 4 h; (g) corresponding acyl chlorides, DMAP, anhydrous DCM, rt, 3 h; (h) CF_3COOH, DCM, rt, 8 h.

methylene group, different substituents on the tetrahydroquinoxaline ring (R^1) were explored. As shown in Table 1, alkoxy groups at the R^1 position showed better potency than hydrogen and electron-withdrawing group fluorine, indicating that electron-donating substitutes at the R^1 position could increase the inhibitory activities. Meanwhile, compounds bearing methoxy were more potent than compounds with ethoxy, demonstrating that the volume of R^1 group was also related with the inhibitory activity. Therefore, the optimal substitute of R^1 was methoxy group. Subsequently, different aromatic fragments at the R^2 position were explored. When R^2 was phenyl group, variable substituents at the C-4 position were investigated. As shown in Table 1, **7e** and **7f** with electron-withdrawing groups could reduce the inhibitory activities, and **7g** with electron-donating group could enhance the inhibitory activity, compared with unsubstituted derivative **7d**. Moving the methoxy group to the C-3 position resulted derivative **7h** which was more potent than **7g**. Replacing the phenyl with naphthyl led to compound **7i** which was less active than **7d**. The ethoxy derivative **7j**, which was unsubstituted in phenyl group, was less active than **7k** with 3,4,5-trimethoxy in phenyl group, illustrating that introduction of electron-donating group such as methoxy was favorable with the inhibitory activity.

Next, replacing the linker methylene group with carbonyl group could significantly improve the antiproliferative activities of the target compounds. Based on the above SAR, methoxy was chosen as R^1 group, and the investigation was focused on the R^2 group. Compound **11a** with 3,4,5-trimethoxyphenyl displayed the most antiproliferative activity with IC_{50} values ranging from 0.16 to 0.18 μM against Hela and HT-29 cell lines. Removing 4-OMe from **11a** produced the derivative **11b**, which maintained activities against both cancer cell lines, implying that 4-OMe was not important for antiproliferative activity. Replacing the methoxy group with the electron-withdrawing group (**11c**) resulted in a dramatic decreased activity. Introducing the saturated or unsaturated ring to the phenyl group resulted derivatives **11d**–**11j**. However, most of these compounds remarkably lost their activities except **11f** and **11g**. **11f** with 4-methoxyl naphthyl exhibited ~5-fold reduced antiproliferative activity compared to that of **11a**, and **11g** bearing 6-quinolinyl was 24-fold more active than **11h** with 5-quinolinyl, and **11g** was only slightly less potent than **11a**. Subsequently, the aromatic group R^2 was then replaced with cyclohexyl or adamantly group. Unfortunately, these modifications were unfavorable to the antiproliferative activities, indicating that the hydrophobic interaction between the aromatic group R^2 and the tubulin played some roles, but the volume, conformation and electronic effect of R^2 were more important for antiproliferative activities.

In summary, compounds **11a** and **11b** exhibited the greatest antiproliferative activities among all the synthetic target compounds. Moreover, compounds **11a** and **11b** were equipotent to the previously reported compounds **12** and **13** against Hela cells, and more active than compounds **12** and **13** against HT-29 cells.

2.2.2. *Tubulin polymerization inhibitory assay*

Based on the antiproliferative activities, compound **11a** was chosen to evaluate its tubulin depolymerization activity in a tubulin polymerization inhibitory assay using purified tubulin. Meanwhile, colchicine was used as the positive control. As shown in Fig. 2, compound **11a** exhibited dose-dependent tubulin polymerization inhibitory activity in a colchicine-like manner, indicating that **11a** was the microtubule-depolymerization agent, and the inhibitory activity of **11a** at 10 μM was comparable to that of CA-4 at 5 μM.

2.2.3. *Immunofluorescence analysis*

Next, immunofluorescence assay in Hela cells was conducted to directly confirm that compound **11a** could inhibit tubulin polymerization dynamics in cellular assay. Hela cells were treated with **11a** at three concentrations (0.15, 0.20 and 0.30 μM) for 24 h, and then stained with Hoechst 33,342 and anti-β-tubulin-Cy3 antibody. As shown in Fig. 3, in the control group, the microtubules were filamentous and extended throughout the cells to maintain the normal cellular morphology. On the contrary, in the experimental groups, the microtubules decreased significantly and solidified around the nucleus in the cells. These results demonstrated that compound **11a** disrupted the microtubule networks in a dose-dependent manner.

2.2.4. *Cell cycle analysis*

The flow cytometry analysis was performed to verify whether compound **11a** could obstruct the cell division and cause cell cycle arrest. Hela cells were treated with compound **11a** at 0.15, 0.20 and 0.25 μM for 24 h, respectively. As presented in Fig. 4, compound **11a** induced a significant decrease in the proportion of cells in the G0/G1 phase and an obvious increase in the proportion of cells in G2/M phase in a dose-

Table 1

In vitro antiproliferative activities of all target compounds.

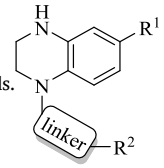

Compd.	R^1	Linker	R^2	MTT assay IC_{50} (μM) [a]	
				Hela	**HT-29**
7a	—H	—CH_2—	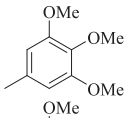	27.93 ± 3.40	35.38 ± 3.90
7b	—F	—CH_2—	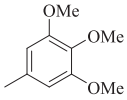	>50	>50
7c	—F	—CH_2—		>50	>50
7d	—OMe	—CH_2—		8.63 ± 2.11	27.14 ± 3.31
7e	—OMe	—CH_2—	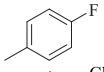	12.20 ± 3.70	11.68 ± 0.73
7f	—OMe	—CH_2—	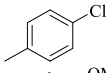	12.92 ± 1.99	7.40 ± 1.74
7g	—OMe	—CH_2—	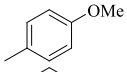	6.00 ± 2.74	9.72 ± 0.39
7h	—OMe	—CH_2—	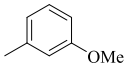	4.17 ± 0.57	4.39 ± 0.53
7i	—OMe	—CH_2—	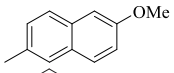	15.00 ± 2.10	17.40 ± 2.20
7j	—OEt	—CH_2—		>50	>50
7k	—OEt	—CH_2—	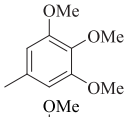	10.32 ± 1.23	12.93 ± 2.68
11a	OMe	—CO—	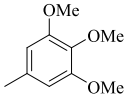	0.16 ± 0.02	0.18 ± 0.03
11b	OMe	—CO—		0.15 ± 0.02	0.20 ± 0.02
11c	OMe	—CO—		11.70 ± 1.92	19.20 ± 2.40
11d	OMe	—CO—		13.40 ± 2.40	12.40 ± 2.50
11e	OMe	—CO—	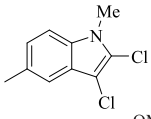	2.38 ± 0.28	2.12 ± 0.30
11f	OMe	—CO—	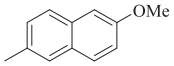	0.87 ± 0.08	1.05 ± 0.09
11g	OMe	—CO—	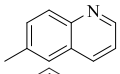	0.36 ± 0.05	0.43 ± 0.05
11h	OMe	—CO—	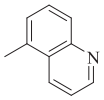	8.57 ± 2.27	10.30 ± 1.98
11i	OMe	—CO—		>50	>50

Table 1 (*continued*)

Compd.	R^1	Linker	R^2	MTT assay IC_{50} (μM) [a]	
				Hela	**HT-29**
11j	OMe	—CO—	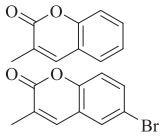	8.94 ± 1.05	8.35 ± 1.02
11k	OMe	—CO—		3.54 ± 0.24	10.79 ± 1.73
11l	OMe	—CO—		13.71 ± 4.38	14.77 ± 0.45
12			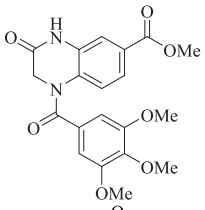	0.126 ± 0.015[b]	1.14 ± 0.39
13			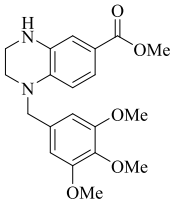	0.194 ± 0.013[c]	0.510 ± 0.036[c]
Colchicine				0.045 ± 0.012	0.25 ± 0.08
CA-4				0.013 ± 0.003	0.013 ± 0.001

[a] IC_{50} values were expressed as the mean ± SD of three independent experiments.
[b] Data were published in Ref. [31].
[c] Data were published in Ref. [32].

dependent manner. When Hela cells were treated with 0.25 μM of compound **11a**, the number of cells in G2/M phase reached 78.3%. These results indicated that compound **11a** could arrest cell cycle at G2/M phase to cause mitotic cell death or mitotic catastrophe.

2.2.5. Cell apoptosis analysis

To determine the influence of compound **11a** on cell death, the cell apoptosis assay was performed in Hela cells. As shown in Fig. 5, compound **11a** induced an important increase in cell apoptosis compared with the control group, in a dose-dependent manner. What's more, the number of apoptotic cells was more than 50% at 0.25 μM. These results indicated that compound **11a** could induce cell apoptosis to treat cancers.

2.2.6. Cytotoxicity evaluation

Compound **11a** was evaluated *in vitro* against human normal LO2 cells to estimate the potential cytotoxicity on non-tumor cell lines. As demonstrated in Table 2, compound **11a** showed lower toxicity toward LO2 cells compared with CA-4.

2.2.7. Molecular docking study

Molecular docking study was performed to understand the interaction of compound **11a** with tubulin. As predicted, **11a** occupied the colchicine binding site and the binding mode was consistent with that of CA-4. As shown in Fig. 6, the 3,4,5-trimethoxyphenyl moiety was accommodated in a hydrophobic pocket, the tetrahydroquinoxaline ring was sandwiched between βN258 and βK352. Additionally, NH from tetrahydroquinoxaline ring formed a hydrogen bond with carbonyl

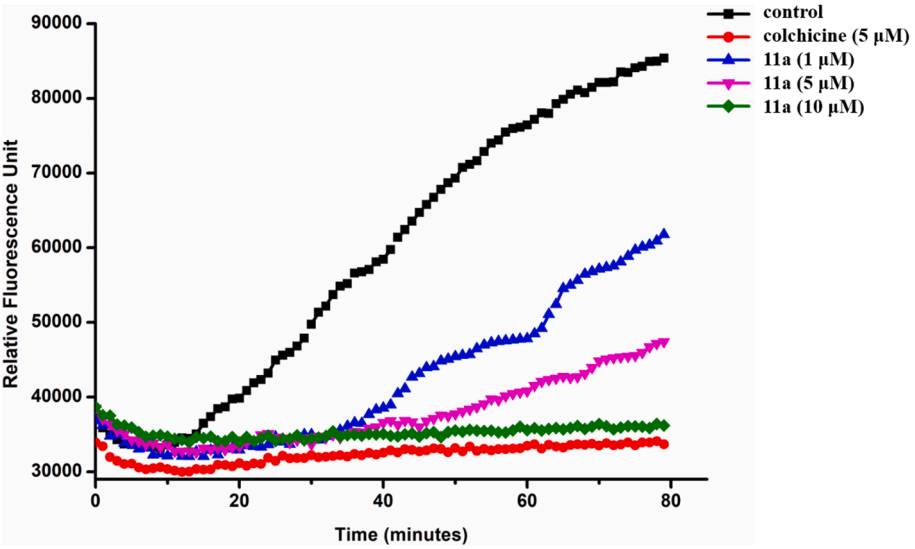

Fig. 2. Effect of **11a** (1, 5 and 10 μM) on tubulin polymerization *in vitro* and colchicine (5 μM) was used as the positive control and 0.1% DMSO was used as the blank control. **11a** (1, 5 or 10 μM), colchicine (5 μM) and 0.1% DMSO were added in a 96-well plate and then polymerizations were detected over 80 min at 37 °C.

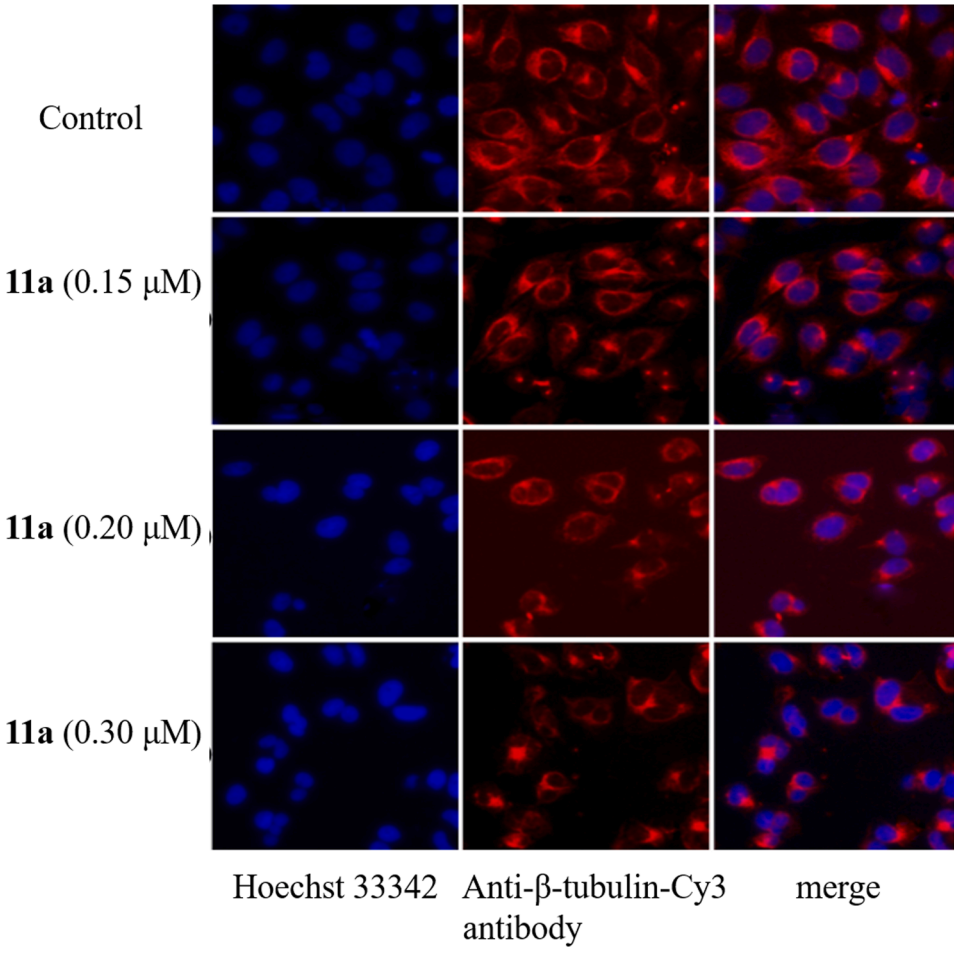

Fig. 3. Images of immunofluorescence staining of microtubules in Hela cells treated with **11a** (0.15, 0.20 or 0.30 μM) for 24 h. Cells were stained with Hoechst 33342 and anti-β-tubulin-Cy3 antibody.

group of αT179.

3. Conclusions

In summary, we have reported the design and synthesis of tetrahydroquinoxaline derivatives as novel colchicine binding site inhibitors.

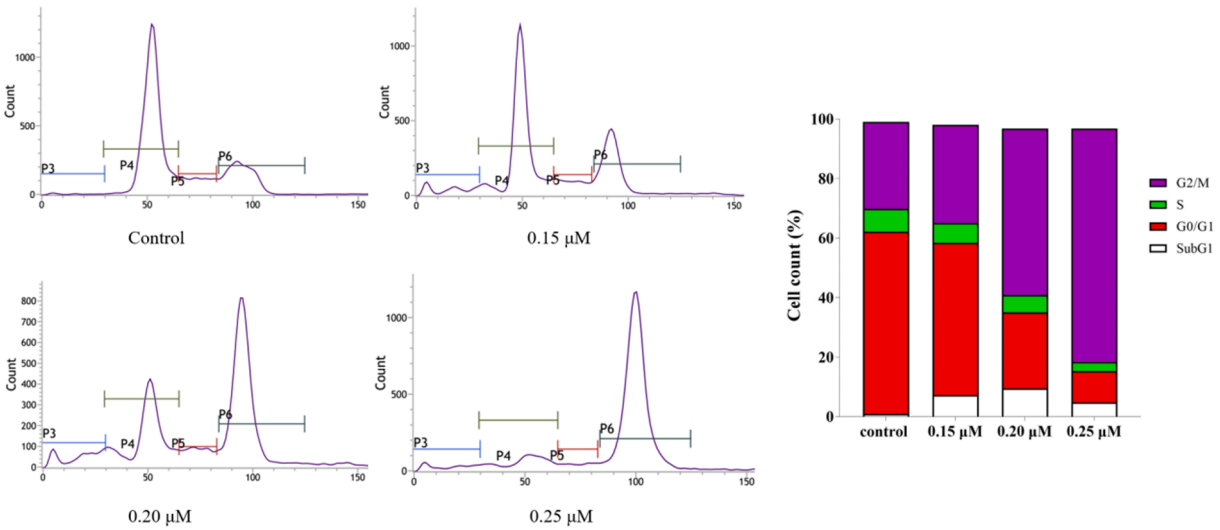

Fig. 4. Compound **11a** arrested cell cycle progression in a dose-dependent manner in Hela cells. (A) Hela cells were treated with **11a** at 0.15, 0.20 and 0.25 μM for 24 h, then analyzed by flow cytometer. (B) The cell cycle distribution.

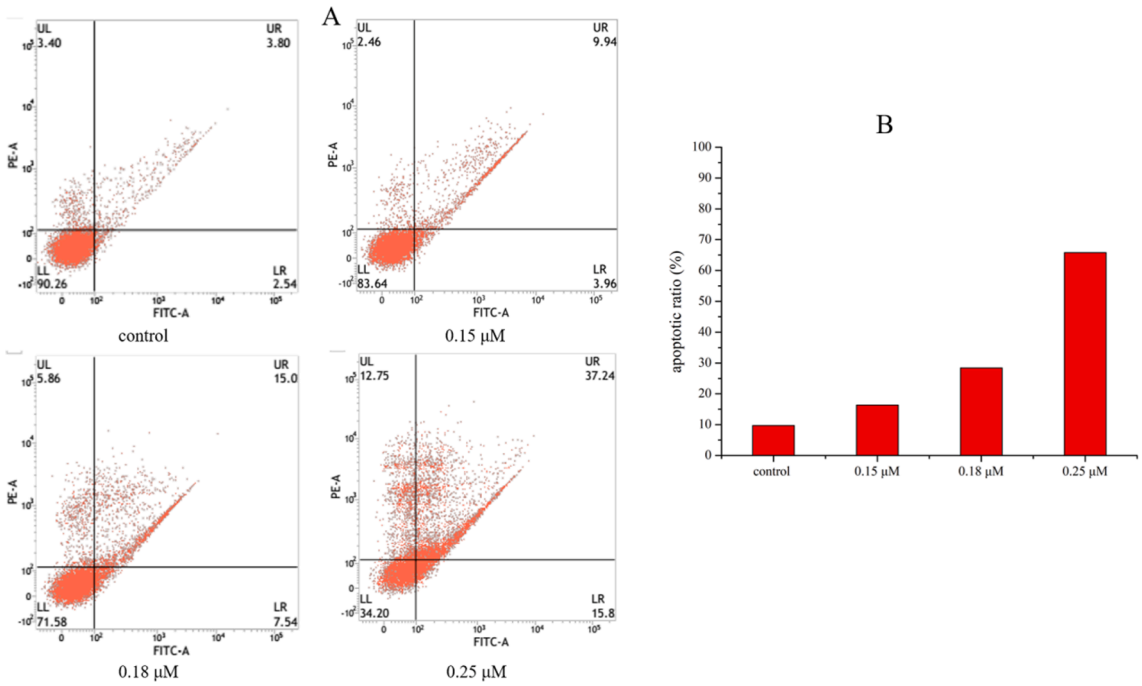

Fig. 5. Effects of compound **11a** to induce apoptosis of Hela cells. (A) Hela cells were treated with **11a** (0.15, 0.18 and 0.25 μM) and DMSO for 24 h, stained with PITC AV and PI, and determined by the flow cytometric analysis. (B) The proportion of apoptotic cells.

Table 2
Antiproliferative activity of **11a** against human normal LO2 cells

Comp.	IC_{50} (μM) [a]
11a	1.22 ± 0.09
CA-4	0.33 ± 0.07[b]

[a] IC_{50} values were expressed as the mean ± SD of three independent experiments.
[b] Data were reported in Ref [33].

The results of cellular assay demonstrated that some of the target compounds showed moderate to strong antiproliferative activities against Hela and HT-29 cell lines. Structure-activity relationships illustrated that the carbonyl derivatives (**11a**–**11l**) were more potent than the methylene derivatives (**7a**–**7k**), and the methoxy on the tetrahydroquinoxaline ring was important for the antiproliferative activity. Among them, compounds **11a** and **11b** showed the strongest antiproliferative activities (**11a**: Hela IC_{50} = 0.16 ± 0.02 μM, HT-29 IC_{50} = 0.18 ± 0.03 μM; **11b**: Hela IC_{50} = 0.15 ± 0.02 μM, HT-29 IC_{50} = 0.20 ± 0.02 μM). The tubulin polymerization inhibitory assay and immunofluorescence analysis suggested that compound **11a** inhibited tubulin polymerization and disturbed the dynamic equilibrium in a colchicine-like manner, indicating **11a** was microtubule depolymerization agent. Further biological studies indicated that **11a** was able to arrest cell cycle in G2/M and induce cell death in a dose-dependent manner. Moreover, **11a** exhibited low toxicity in normal LO2 cells in comparison to tumor cells. Besides these, molecular docking study demonstrated that

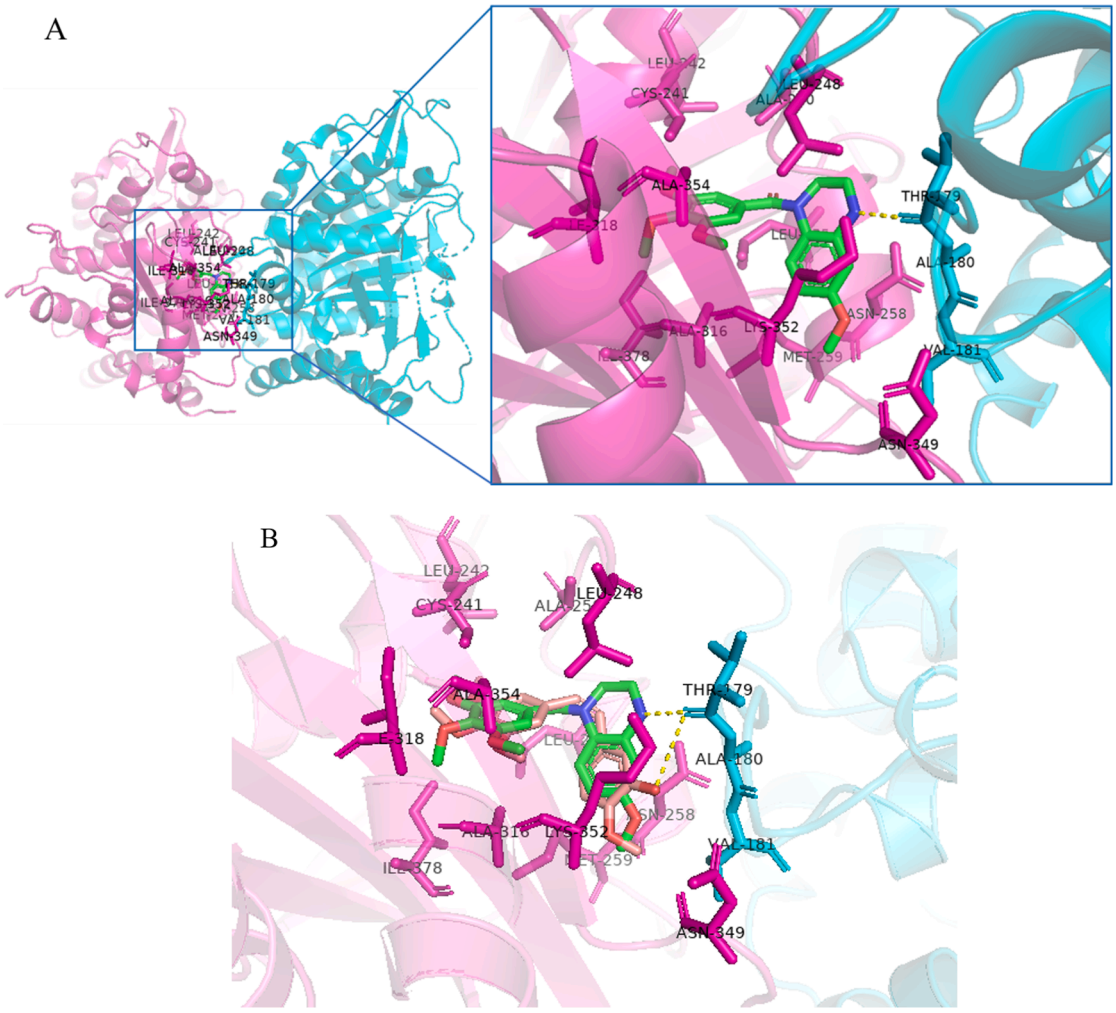

Fig. 6. (A) Proposed binding mode of compound **11a** with the colchicine binding site (PDB: 5LYJ). (B) Overlap of the structures of **11a** (green) and CA-4 (pink). (For interpretation of the references to colour in this figure legend, the reader is referred to the web version of this article.)

compound **11a** acted on the colchicine binding site. Therefore, compound **11a** was a promising drug candidate targeting colchicine binding site for further development.

4. Experimental sections

4.1. Chemistry

4.1.1. General materials and methods

All the materials were obtained commercially and used without further purification unless noted otherwise. All solvents were analytical purity. Reactions were monitored by thin layer chromatography (TLC) by UV absorbance (254 nm). Flash column chromatography were performed on silica gel (100–200 mesh, 200–300 mesh). Melting points were determined by hot-stage microscope (SGW X-4) and the instrument was uncorrected. NMR spectra were recorded on Bruker ADVANCE 300 (^{1}H NMR: 300 MHz, ^{13}C NMR: 75 MHz) and referenced to deuterium dimethyl sulfoxide (DMSO-d_6) or deuterium chloroform ($CDCl_3$). The coupling constants J were given in Hz, and the abbreviations were used to describe peak patterns where appropriate: singlet (s), doublet (d), triplet (t), multiplet (m), broad resonances (br). High-resolution mass spectrometry (HRMS) were acquired via a Thermo Scientific LTQ Orbitrap XL mass spectrometer. The purities of all target compounds were determined by reverse-phase HPLC using a Waters Alliance e2695 series LC system (column, XBridge® C18, 4.6 mm × 150 mm, 5 μm; mobile phase, methanol/buffer solution (3.56 g Na_2HPO_4 + 1.56 g NaH_2PO_4 + 1000 mL H_2O); temperature: 35 °C, flow rate, 1.0 mL/min; UV wavelength, 254 nm), gradient elution: 0–1 min (methanol 25%), 1–5 min (methanol 25%-75%), 5–18 min (methanol 75%), 18–22 min (methanol 75%-25%), 22–23 min (methanol 25%).

4.1.2. Synthesis of 4-fluoro-2-nitro-N-(3,4,5-trimethoxybenzyl)aniline (4a)

To a solution of 4-fluoro-2-nitroaniline (1.50 g, 9.61 mmol) in acetonitrile (30 mL) was added anhydrous K_2CO_3 (3.19 g, 23.06 mmol), KI (1.59 g, 9.61 mmol) and 5-(chloromethyl)-1,2,3-trimethoxybenzene (4.16 g, 19.22 mmol). The mixture was stirred at 70 °C for 6 h. After completion, the mixture was cooled to room temperature, and the solvent was evaporated under reduced pressure. The crude product was purified by column chromatography (PE:EA = 20:1) to obtain **4a** (2.00 g, 61.9%) as an orange solid. m.p.: 97–98 °C. ^{1}H NMR (300 MHz, $CDCl_3$) δ 8.26 (br, 1H), 7.91 (dd, J = 9.1, 2.9 Hz, 1H), 7.26–7.16 (m, 1H), 6.80 (dd, J = 9.4, 4.5 Hz, 1H), 6.56 (s, 2H), 4.46 (d, J = 5.4 Hz, 2H), 3.84 (s, 9H). MS (ESI) $[M+H]^+$ 337.01.

Compounds **4b**–**4j** and **5a** were synthesized following a similar method of compound **4a**.

4.1.3. Synthesis of 4-fluoro-N-(3-methoxybenzyl)-2-nitroaniline (4b)

Orange-red oil (58.9%). ^{1}H NMR (300 MHz, $CDCl_3$) δ 8.34 (br, 1H), 7.92 (dd, J = 9.2, 3.0 Hz, 1H), 7.29 (t, J = 7.1 Hz, 1H), 7.17 (d, J = 7.4 Hz, 1H), 6.92 (d, J = 7.4 Hz, 1H), 6.85 (d, J = 9.0 Hz, 2H), 6.79 (d, J = 4.6 Hz, 1H), 4.52 (d, J = 5.7 Hz, 2H), 3.80 (s, 3H). MS (ESI) $[M+H]^+$

278.09.

*4.1.4. Synthesis of N-benzyl-4-methoxy-2-nitroaniline **(4c)***

Orange solid (65.0%). m.p.: 94–95 °C. ^{1}H NMR (300 MHz, $CDCl_3$) δ 8.37 (s, 1H), 7.65 (d, J = 2.9 Hz, 1H), 7.42–7.28 (m, 5H), 7.09 (dd, J = 9.3, 2.8 Hz, 1H), 6.78 (d, J = 9.4 Hz, 1H), 4.55 (d, J = 5.8 Hz, 2H), 3.79 (s, 3H). MS (ESI) $[M+H]^+$ 258.95.

*4.1.5. Synthesis of N-(4-fluorobenzyl)-4-methoxy-2-nitroaniline **(4d)***

Red solid (78.5%). m.p.: 66–67 °C. ^{1}H NMR (300 MHz, $CDCl_3$) δ 8.33 (s, 1H), 7.65 (d, J = 2.9 Hz, 1H), 7.34–7.28 (m, 2H), 7.14–7.06 (m, 3H), 6.75 (d, J = 9.4 Hz, 1H), 4.52 (d, J = 5.7 Hz, 2H), 3.79 (s, 3H). MS (ESI) $[M+H]^+$ 275.13.

*4.1.6. Synthesis of N-(4-chlorobenzyl)-4-methoxy-2-nitroaniline **(4e)***

Red solid (75.3%). m.p.: 76–78 °C. ^{1}H NMR (300 MHz, $CDCl_3$) δ 8.34 (s, 1H), 7.65 (d, J = 3.0 Hz, 1H), 7.33 (d, J = 8.5 Hz, 2H), 7.27 (d, J = 6.5 Hz, 2H), 7.09 (dd, J = 9.3, 3.0 Hz, 1H), 6.71 (d, J = 9.3 Hz, 1H), 4.52 (d, J = 5.8 Hz, 2H), 3.79 (s, 3H). MS (ESI) $[M+H]^+$ 293.45.

*4.1.7. Synthesis of 4-methoxy-N-(4-methoxybenzyl)-2-nitroaniline **(4f)***

Red solid (91.0%). m.p.: 75–76 °C. ^{1}H NMR (300 MHz, $CDCl_3$) δ 8.30 (s, 1H), 7.63 (d, J = 3.0 Hz, 1H), 7.27–7.26 (m, 1H), 7.25–7.23 (m, 1H), 7.09 (dd, J = 9.4, 3.0 Hz, 1H), 6.91–6.89 (m, 1H), 6.88–6.86 (m, 1H), 6.79 (d, J = 9.4 Hz, 1H), 4.46 (s, 2H), 3.80 (s, 3H), 3.78 (s, 3H). MS (ESI) $[M+H]^+$ 290.09.

*4.1.8. Synthesis of 4-methoxy-N-(3-methoxybenzyl)-2-nitroaniline **(4g)***

Red solid (75.9%). m.p.: 65–66 °C. ^{1}H NMR (300 MHz, $CDCl_3$) δ 8.38 (s, 1H), 7.65 (s, 1H), 7.29 (t, J = 6.0 Hz, 1H), 7.09 (d, J = 9.4 Hz, 1H), 6.92 (d, J = 7.5 Hz, 1H), 6.87 (s, 1H), 6.83 (d, J = 8.1 Hz, 1H), 6.77 (d, J = 9.4 Hz, 1H), 4.52 (d, J = 5.7 Hz, 2H), 3.80 (s, 3H), 3.79 (s, 3H). MS (ESI) $[M+H]^+$ 288.96.

*4.1.9. Synthesis of 4-methoxy-N-((6-methoxynaphthalen-2-yl)methyl)-2-nitroaniline **(4h)***

Red solid (74.0%). m.p.: 79–80 °C. ^{1}H NMR (300 MHz, $CDCl_3$) δ 8.45 (s, 1H), 7.77–7.61 (m, 4H), 7.41 (d, J = 8.5 Hz, 1H), 7.19–7.14 (m, 1H), 7.14 (s, 1H), 7.07 (d, J = 9.3 Hz, 1H), 6.83 (d, J = 9.4 Hz, 1H), 4.68 (s, 2H), 3.92 (s, 3H), 3.78 (s, 3H). MS (ESI) $[M+H]^+$ 340.21.

*4.1.10. Synthesis of N-benzyl-4-ethoxy-2-nitroaniline **(4i)***

Red solid (78.9%). m.p.: 65–66 °C. ^{1}H NMR (300 MHz, $CDCl_3$) δ 8.35 (s, 1H), 7.63 (s, 1H), 7.39–7.28 (m, 5H), 7.09 (d, J = 9.4 Hz, 1H), 6.77 (d, J = 9.3 Hz, 1H), 4.54 (d, J = 5.7 Hz, 2H), 3.99 (q, J = 7.0 Hz, 2H), 1.39 (t, J = 7.0 Hz, 3H). MS (ESI) $[M+H]^+$ 274.12.

*4.1.11. Synthesis of 4-ethoxy-2-nitro-N-(3,4,5-trimethoxybenzyl)aniline **(4j)***

Red solid (75.3%). m.p.: 100–101 °C. ^{1}H NMR (300 MHz, $CDCl_3$) δ 7.41 (s, 1H), 7.37 (s, 1H), 6.62 (s, 2H), 6.58 (d, J = 8.8 Hz, 1H), 6.40 (d, J = 8.9 Hz, 1H), 3.94–3.91 (m, 4H), 3.84 (s, 3H), 3.76 (s, 3H), 3.69 (s, 6H). MS (ESI) $[M+H]^+$ 362.07.

*4.1.12. Synthesis of N^1-(3,4,5-trimethoxybenzyl)benzene-1,2-diamine **(5a)***

Following similar procedure to that described for preparing **4a**, compound **5a** was obtained from benzene-1,2-diamine **3a** (1.50 g, 13.87 mmol), anhydrous K_2CO_3 (4.60 g, 33.29 mmol), KI (2.30 g, 13.87 mmol) and 5-(chloromethyl)-1,2,3-trimethoxybenzene (6.01 g, 27.74 mmol) as a brown solid (54.3%). m.p.: 123–125 °C. ^{1}H NMR (300 MHz, $CDCl_3$) δ 6.82 (td, J = 7.2, 1.2 Hz, 1H), 6.76–6.67 (m, 3H), 6.64 (s, 2H), 4.24 (s, 2H), 3.85 (s, 9H). HRMS (ESI) *m/z*: calcd for $C_{16}H_{20}N_2O_3Na^+$ $[M + Na]^+$ 311.13661, found 311.13608.

*4.1.13. Synthesis of 4-fluoro-N^1-(3,4,5-trimethoxybenzyl)benzene-1,2-diamine **(5b)***

To a solution of **4a** (1.50 g, 4.46 mmol) in MeOH (25 mL) was added 10% Pd/C (0.23 g, 0.22 mmol), and the reaction mixture was stirred at room temperature under H_2 atmosphere. After completion, the mixture was filtered with Celite, and the filtrate was concentrated under vacuum to give **5b** (0.95 g, 69.8%) as an orange solid. m.p.: 117–118 °C. ^{1}H NMR (300 MHz, $CDCl_3$) δ 6.62 (s, 2H), 6.60–6.56 (m, 1H), 6.48 (d, J = 8.9 Hz, 2H), 4.18 (s, 2H), 3.85 (s, 9H), 3.56 (s, 2H), 3.30 (s, 1H). MS (ESI) $[M+H]^+$ 306.97.

Compounds **5c**–**5k** were synthesized following a similar method of compound **5b**.

*4.1.14. Synthesis of 4-fluoro-N^1-(3-methoxybenzyl)benzene-1,2-diamine **(5c)***

Reddish-brown solid (58.8%). m.p.: 108–109 °C. ^{1}H NMR (300 MHz, $CDCl_3$) δ 7.29 (d, J = 7.8 Hz, 1H), 6.97 (d, J = 7.9 Hz, 1H), 6.94 (s, 1H), 6.84 (d, J = 8.2 Hz, 1H), 6.58 (dd, J = 8.3, 5.4 Hz, 1H), 6.53–6.38 (m, 2H), 4.23 (s, 2H), 3.81 (s, 3H), 3.57 (s, 2H), 3.33 (s, 1H). MS (ESI) $[M+H]^+$ 246.93.

*4.1.15. Synthesis of N^1-benzyl-4-methoxybenzene-1,2-diamine **(5d)***

Pale yellow oil (26.1%). ^{1}H NMR (300 MHz, $CDCl_3$) δ 7.44–7.27 (m, 5H), 6.63 (d, J = 8.5 Hz, 1H), 6.37 (s, 1H), 6.32 (d, J = 8.5 Hz, 1H), 4.24 (s, 2H), 3.73 (s, 3H), 3.55 (s, 2H), 3.19 (s, 1H). MS (ESI) $[M+H]^+$ 228.93.

*4.1.16. Synthesis of N^1-(4-fluorobenzyl)-4-methoxybenzene-1,2-diamine **(5e)***

Red oil (35.8%). ^{1}H NMR (300 MHz, $CDCl_3$) δ 7.38–7.31 (m, 2H), 7.06–6.98 (m, 2H), 6.59 (d, J = 8.5 Hz, 1H), 6.37 (s, 1H), 6.32 (d, J = 8.4 Hz, 1H), 4.21 (s, 2H), 3.73 (s, 3H), 3.55 (s, 2H), 3.20 (s, 1H). MS (ESI) $[M+H]^+$ 246.94.

*4.1.17. Synthesis of N^1-(4-chlorobenzyl)-4-methoxybenzene-1,2-diamine **(5f)***

White solid (34.9%). m.p.: 81–82 °C. ^{1}H NMR (300 MHz, $CDCl_3$) δ 7.31 (br, 4H), 6.56 (d, J = 8.5 Hz, 1H), 6.36 (s, 1H), 6.30 (d, J = 8.5 Hz, 1H), 4.22 (s, 2H), 3.73 (s, 3H), 3.55 (s, 2H), 3.22 (s, 1H). MS (ESI) $[M+H]^+$ 263.86.

*4.1.18. Synthesis of 4-methoxy-N^1-(4-methoxybenzyl)benzene-1,2-diamine **(5g)***

Pale pink solid (35.7%). m.p.: 87–88 °C. ^{1}H NMR (300 MHz, $CDCl_3$) δ 7.31 (d, J = 8.4 Hz, 2H), 6.88 (d, J = 8.5 Hz, 2H), 6.63 (d, J = 8.4 Hz, 1H), 6.36 (s, 1H), 6.33 (d, J = 8.4 Hz, 1H), 4.16 (s, 2H), 3.81 (s, 3H), 3.73 (s, 3H), 3.54 (s, 2H), 3.12 (s, 1H). MS (ESI) $[M+H]^+$ 258.94.

*4.1.19. Synthesis of 4-methoxy-N^1-(3-methoxybenzyl)benzene-1,2-diamine **(5h)***

Red oil (45.2%). ^{1}H NMR (300 MHz, $CDCl_3$) δ 7.23 (t, J = 7.6 Hz, 1H), 6.97 (d, J = 6.0 Hz, 1H), 6.95 (s, 1H), 6.81 (d, J = 8.3 Hz, 1H), 6.60 (d, J = 8.4 Hz, 1H), 6.34 (s, 1H), 6.30 (d, J = 8.4 Hz, 1H), 4.19 (s, 2H), 3.78 (s, 3H), 3.71 (s, 3H), 3.42 (s, 3H). MS (ESI) $[M+H]^+$ 258.93.

*4.1.20. Synthesis of 4-methoxy-N^1-((6-methoxynaphthalen-2-yl)methyl) benzene-1,2-diamine **(5i)***

Reddish solid (60.6%). m.p.: 84–85 °C. ^{1}H NMR (300 MHz, $CDCl_3$) δ 7.79–7.69 (m, 3H), 7.49 (d, J = 8.3 Hz, 1H), 7.15 (d, J = 7.0 Hz, 2H), 6.67 (d, J = 8.5 Hz, 1H), 6.38 (s, 1H), 6.32 (d, J = 8.5 Hz, 1H), 4.37 (s, 2H), 3.93 (s, 3H), 3.73 (s, 3H), 3.56 (s, 2H), 3.20 (s, 1H). MS (ESI) $[M + 1]^+$ 309.03.

*4.1.21. Synthesis of N^1-benzyl-4-ethoxybenzene-1,2-diamine **(5j)***

Reddish-brown oil (37.2%). ^{1}H NMR (300 MHz, $CDCl_3$) δ 7.42–7.27 (m, 5H), 6.62 (d, J = 8.6 Hz, 1H), 6.37 (s, 1H), 6.32 (d, J = 8.4 Hz, 1H),

4.24 (s, 2H), 3.95 (q, $J = 6.9$ Hz, 2H), 3.53 (s, 2H), 3.19 (s, 1H), 1.37 (t, $J = 7.0$ Hz, 3H). MS (ESI) $[M+H]^+$ 242.94.

4.1.22. Synthesis of 4-ethoxy-N^1-(3,4,5-trimethoxybenzyl)benzene-1,2-diamine (5k)

Red solid (73.8%). m.p.: 127–128 °C. ^{1}H NMR (300 MHz, $CDCl_3$) δ 6.64–6.60 (m, 3H), 6.38 (d, $J = 2.6$ Hz, 1H), 6.33 (dd, $J = 8.5$, 2.6 Hz, 1H), 4.16 (s, 2H), 3.95 (q, $J = 7.0$ Hz, 2H), 3.85 (s, 6H), 3.85 (s, 3H), 3.53 (s, 2H), 3.18 (s, 1H), 1.37 (t, $J = 7.0$ Hz, 3H). MS (ESI) $[M+H]^+$ 333.09.

4.1.23. Synthesis of 1-(3,4,5-trimethoxybenzyl)-1,4-dihydroquinoxaline-2,3-dione (6a)

5a (1.00 g, 3.47 mmol) and dimethyl oxalate (4.10 g, 34.68 mmol) were added to 100 mL round-bottom flask, and the reaction mixture was stirred at 70 °C for 5 h. Then the mixture was cooled to room temperature, diluted with anhydrous ether (50 mL) and stirred for 30 min, then the precipitate was filtered to obtain **6a** (0.92 g, 77.3%) as a gray solid. m.p.: 234–236 °C. ^{1}H NMR (300 MHz, $CDCl_3$) δ 11.35 (br, 1H), 7.37 (dd, $J = 7.2$, 2.1 Hz, 1H), 7.27–7.26 (m, 3H), 6.54 (s, 2H), 5.40 (s, 2H), 3.81 (s, 9H). HRMS (ESI) *m/z*: calcd for $C_{18}H_{19}N_2O_5Na^+$ $[M + Na]^+$ 365.11079, found 365.11108.

Compounds **6b**–**6k** were synthesized following a similar method of compound **6a**.

4.1.24. Synthesis of 6-fluoro-1-(3,4,5-trimethoxybenzyl)-1,4-dihydroquinoxaline-2,3-dione (6b)

White solid (65.3%). m.p.: 223–224 °C. ^{1}H NMR (300 MHz, $CDCl_3$) δ 11.55 (s, 1H), 7.22–7.12 (m, 2H), 6.94–6.87 (m, 1H), 6.51 (s, 2H), 5.38 (s, 2H), 3.82 (s, 9H). MS (ESI) $[M+H]^+$ 362.24.

4.1.25. Synthesis of 6-fluoro-1-(3-methoxybenzyl)-1,4-dihydroquinoxaline-2,3-dione (6c)

White solid (83.3%). m.p.: 174–175 °C. ^{1}H NMR (300 MHz, $CDCl_3$) δ 11.84 (s, 1H), 7.28 (d, $J = 7.0$ Hz, 1H), 7.19–7.09 (m, 2H), 6.86–6.81 (m, 4H), 5.43 (s, 2H), 3.77 (s, 3H). MS (ESI) $[M+H]^+$ 302.12.

4.1.26. Synthesis of 1-benzyl-6-methoxy-1,4-dihydroquinoxaline-2,3-dione (6d)

White solid (65.8%). m.p.: 142–143 °C. ^{1}H NMR (300 MHz, $CDCl_3$) δ 11.13 (s, 1H), 7.38–7.27 (m, 5H), 7.07 (d, $J = 9.2$ Hz, 1H), 6.82 (s, 1H), 6.70 (d, $J = 9.1$ Hz, 1H), 5.45 (s, 2H), 3.81 (s, 3H). MS (ESI) $[M+H]^+$ 281.98.

4.1.27. Synthesis of 1-(4-fluorobenzyl)-6-methoxy-1,4-dihydroquinoxaline-2,3-dione (6e)

White solid (78.2%). m.p.: 152–153 °C. ^{1}H NMR (300 MHz, $CDCl_3$) δ 11.61 (s, 1H), 7.29 (d, $J = 8.5$ Hz, 2H), 7.03 (d, $J = 8.5$ Hz, 2H), 7.00 (d, $J = 8.8$ Hz, 1H), 6.91 (s, 1H), 6.70 (d, $J = 8.8$ Hz, 1H), 5.39 (s, 2H), 3.81 (s, 3H). MS (ESI) $[M+H]^+$ 300.96.

4.1.28. Synthesis of 1-(4-chlorobenzyl)-6-methoxy-1,4-dihydroquinoxaline-2,3-dione (6f)

White solid (77.5%). m.p.: 125–126 °C. ^{1}H NMR (300 MHz, $CDCl_3$) δ 11.45 (s, 1H), 7.30 (d, $J = 8.4$ Hz, 2H), 7.22 (d, $J = 8.4$ Hz, 2H), 7.00 (d, $J = 9.1$ Hz, 1H), 6.90 (s, 1H), 6.69 (d, $J = 8.6$ Hz, 1H), 5.39 (s, 2H), 3.81 (s, 3H). MS (ESI) $[M+H]^+$ 318.20.

4.1.29. Synthesis of 6-methoxy-1-(4-methoxybenzyl)-1,4-dihydroquinoxaline-2,3-dione (6g)

White solid (69.2%). m.p.: 166–167 °C. ^{1}H NMR (300 MHz, $CDCl_3$) δ 11.06 (s, 1H), 7.22 (d, $J = 8.6$ Hz, 2H), 7.12 (d, $J = 9.2$ Hz, 1H), 6.85 (d, $J = 8.6$ Hz, 2H), 6.80 (s, 1H), 6.71 (d, $J = 9.2$ Hz, 1H), 5.38 (s, 2H), 3.81 (s, 3H), 3.77 (s, 3H). MS (ESI) $[M+H]^+$ 312.96.

4.1.30. Synthesis of 6-methoxy-1-(3-methoxybenzyl)-1,4-dihydroquinoxaline-2,3-dione (6h)

White solid (59.3%). m.p.: 175–176 °C. ^{1}H NMR (300 MHz, $CDCl_3$) δ 11.36 (s, 1H), 7.25–7.19 (m, 1H), 7.07 (d, $J = 8.8$ Hz, 1H), 6.95–6.77 (m, 4H), 6.69 (d, $J = 8.6$ Hz, 1H), 5.41 (s, 2H), 3.81 (s, 3H), 3.77 (s, 3H). MS (ESI) $[M+H]^+$ 313.00.

4.1.31. Synthesis of 6-methoxy-1-((6-methoxynaphthalen-2-yl)methyl)-1,4-dihydroquinoxaline-2,3-dione (6i)

White solid (44.8%). m.p.: 137–138 °C. ^{1}H NMR (300 MHz, $CDCl_3$) δ 11.74 (s, 1H), 7.70 (d, $J = 8.5$ Hz, 1H), 7.66 (d, $J = 8.5$ Hz, 1H), 7.63 (s, 1H), 7.38 (d, $J = 8.4$ Hz, 1H), 7.12 (d, $J = 9.4$ Hz, 2H), 7.09 (s, 1H), 6.90 (s, 1H), 6.66 (d, $J = 9.1$ Hz, 1H), 5.55 (s, 2H), 3.89 (s, 3H), 3.76 (s, 3H). MS (ESI) $[M+H]^+$ 361.03.

4.1.32. Synthesis of 1-benzyl-6-ethoxy-1,4-dihydroquinoxaline-2,3-dione (6j)

White solid (53.8%). m.p.: 193–195 °C. ^{1}H NMR (300 MHz, $CDCl_3$) δ 11.92 (s, 1H), 7.39–7.26 (m, 5H), 7.04 (d, $J = 9.2$ Hz, 1H), 6.91 (s, 1H), 6.68 (d, $J = 9.2$ Hz, 1H), 5.44 (s, 2H), 4.01 (q, $J = 6.5$ Hz, 2H), 1.38 (t, $J = 6.7$ Hz, 3H). MS (ESI) $[M+H]^+$ 296.98.

4.1.33. Synthesis of 6-ethoxy-1-(3,4,5-trimethoxybenzyl)-1,4-dihydroquinoxaline-2,3-dione (6k)

White solid (65.3%). m.p.: 258–260 °C. ^{1}H NMR (300 MHz, $CDCl_3$) δ 11.05 (s, 1H), 7.12 (d, $J = 9.1$ Hz, 1H), 6.81 (s, 1H), 6.73 (d, $J = 9.1$ Hz, 1H), 6.51 (s, 2H), 5.36 (s, 2H), 4.03 (q, $J = 6.9$ Hz, 2H), 3.81 (s, 9H), 1.41 (t, $J = 7.0$ Hz, 3H). MS (ESI) $[M+H]^+$ 386.03.

4.1.34. Synthesis of 1-(3,4,5-trimethoxybenzyl)-1,2,3,4-tetrahydroquinoxaline (7a)

In a two-necked flask equipped with a dropping funnel under nitrogen, **6a** (0.85 g, 2.48 mmol) was dissolved in anhydrous THF (15 mL), and the mixture was cooled to 0 °C and stirred for 15 min. Then borane-tetrahydrofuran complex (1 mol /L, 4.90 mL) was added to the mixture dropwise during 30 min. The mixture reaction was then stirred at room temperature overnight. Then the mixture was cooled to 0 °C and water was added until no gas was formed and stirred for 20 min. The mixture was extracted with DCM, and the organic layer was dried over anhydrous Na_2SO_4, filtered. The filtrate was concentrated and purified by chromatography (PE:EA = 10:1) to afford **7a** (0.64 g, 82.3%) as a white solid. HPLC purity: 95.54%, retention time: 8.23 min. m.p.: 109–111 °C. ^{1}H NMR (300 MHz, $CDCl_3$) δ 6.64–6.57 (m, 3H), 6.54 (s, 3H), 4.35 (s, 2H), 3.84 (s, 3H), 3.82 (s, 6H), 3.44 (t, $J = 4.8$ Hz, 2H), 3.36 (t, $J = 4.8$ Hz, 2H). ^{13}C NMR (75 MHz, $CDCl_3$) δ 153.6, 137.0, 135.7, 134.7, 134.2, 119.3, 118.2, 114.2, 112.3, 103.9, 61.0, 56.3, 55.9, 48.3, 41.3. HRMS (ESI) *m/z*: calcd for $C_{18}H_{22}N_2O_3Na^+$ $[M+H]^+$ 337.15226, found 337.15244.

Compounds **7b**–**7k** were synthesized following a similar method of compound **7a**.

4.1.35. Synthesis of 6-fluoro-1-(3,4,5-trimethoxybenzyl)-1,2,3,4-tetrahydroquinoxaline (7b)

Colorless oil (79.3%). HPLC purity: 96.05%, retention time: 8.04 min. ^{1}H NMR (300 MHz, $CDCl_3$) δ 6.54 (s, 2H), 6.46 (dd, $J = 8.4$, 5.5 Hz, 1H), 6.31–6.20 (m, 2H), 4.26 (s, 2H), 3.91 (br, 1H), 3.84 (s, 3H), 3.82 (s, 6H), 3.43 (s, 2H), 3.24 (s, 2H). ^{13}C NMR (75 MHz, $CDCl_3$) δ 158.13, 155.02, 153.47, 136.78, 135.58 (d, $J_{F\text{-}C} = 10.2$ Hz), 134.45, 131.47 (d, $J_{F\text{-}C} = 1.7$ Hz), 112.99 (d, $J_{F\text{-}C} = 9.0$ Hz), 103.92, 103.56, 100.78 (d, $J_{F\text{-}C} = 25.9$ Hz), 60.89, 56.47, 56.11, 47.53, 41.09. HRMS (ESI) *m/z* calcd for $C_{18}H_{22}FN_2O_3^+$ $[M+H]^+$ 333.16090, found 333.16098.

4.1.36. Synthesis of 6-fluoro-1-(3-methoxybenzyl)-1,2,3,4-tetrahydroquinoxaline (7c)

Colorless oil (61.4%). HPLC purity: 95.12%, retention time: 9.28 min. ^{1}H NMR (300 MHz, $CDCl_3$) δ 7.29–7.24 (m, 1H), 6.91 (d, $J = 8.3$

Hz, 1H), 6.87 (s, 1H), 6.80 (d, $J = 8.0$ Hz, 1H), 6.44–6.38 (t, $J = 9.0$ Hz, 1H), 6.28 (d, $J = 7.2$ Hz, 1H), 6.23 (s, 1H), 4.33 (s, 2H), 3.84 (br, 1H), 3.79 (s, 3H), 3.45 (t, $J = 4.0$ Hz, 2H), 3.30 (t, $J = 4.0$ Hz, 2H). ^{13}C NMR (75 MHz, $CDCl_3$) δ 160.02, 158.00, 154.90, 140.56, 135.44 (d, $J_{F\text{-}C} = 10.1$ Hz), 131.51 (d, $J_{F\text{-}C} = 1.7$ Hz), 129.75, 119.56, 112.88, 112.69 (d, $J_{F\text{-}C} = 9.1$ Hz), 103.80 (d, $J_{F\text{-}C} = 21.8$ Hz), 100.84 (d, $J_{F\text{-}C} = 25.9$ Hz), 56.12, 55.25, 47.88, 41.11. HRMS (ESI) *m/z* calcd for $C_{16}H_{18}FN_2O^+$ $[M+H]^+$ 273.13977, found 273.13995.

4.1.37. Synthesis of 1-benzyl-6-methoxy-1,2,3,4-tetrahydroquinoxaline (7d)

White solid (64.3%). HPLC purity: 95.26%, retention time: 8.11 min. m.p.: 89–91 °C. ^{1}H NMR (300 MHz, $CDCl_3$) δ 7.36–7.29 (m, 4H), 7.26–7.20 (m, 1H), 6.48 (d, $J = 8.7$ Hz, 1H), 6.30–6.08 (m, 2H), 4.34 (s, 2H), 3.70 (s, 3H), 3.44 (s, 2H), 3.27 (s, 2H). ^{13}C NMR (75 MHz, $CDCl_3$) δ 152.94, 139.16, 135.60, 129.83, 128.65, 127.48, 127.00, 113.55, 102.96, 101.07, 56.52, 55.63, 48.06, 41.20. HRMS (ESI) *m/z* calcd for $C_{16}H_{19}N_2O^+$ $[M+H]^+$ 255.14919, found 255.14946.

4.1.38. Synthesis of 1-(4-fluorobenzyl)-6-methoxy-1,2,3,4-tetrahydroquinoxaline (7e)

White solid (26.5%). HPLC purity: 97.21%, retention time: 8.82 min. m.p.: 90–91 °C. ^{1}H NMR (300 MHz, $CDCl_3$) δ 7.33–7.25 (m, 2H), 7.00 (t, $J = 8.6$ Hz, 2H), 6.45 (d, $J = 8.8$ Hz, 1H), 6.22–6.11 (m, 2H), 4.29 (s, 2H), 3.79 (s, 1H), 3.69 (s, 3H), 3.42 (s, 2H), 3.24 (s, 2H). ^{13}C NMR (75 MHz, $CDCl_3$) δ 163.58, 160.34, 153.00, 135.60, 129.59, 128.90 (d, $J_{F\text{-}C} = 7.9$ Hz), 115.43 (d, $J_{F\text{-}C} = 21.3$ Hz), 113.59, 102.96, 101.06, 55.89, 55.63, 48.05, 41.19. HRMS (ESI) *m/z* calcd for $C_{16}H_{18}FN_2O^+$ $[M+H]^+$ 273.13977, found 273.13995.

4.1.39. Synthesis of 1-(4-chlorobenzyl)-6-methoxy-1,2,3,4-tetrahydroquinoxaline (7f)

White solid (27.8%). HPLC purity: 97.23%, retention time: 8.80 min. m.p.: 108–110 °C. ^{1}H NMR (300 MHz, $CDCl_3$) δ 7.33–7.26 (m, 4H), 6.41 (d, $J = 8.8$ Hz, 1H), 6.23–6.09 (m, 2H), 4.30 (s, 2H), 3.77 (s, 1H), 3.70 (s, 3H), 3.44 (s, 2H), 3.26 (s, 2H). ^{13}C NMR (75 MHz, $CDCl_3$) δ 153.04, 137.67, 135.55, 132.56, 129.41, 128.73, 113.57, 102.99, 101.06, 55.96, 55.58, 48.18, 41.14. HRMS (ESI) *m/z* calcd for $C_{16}H_{18}ClN_2O^+$ $[M+H]^+$ 289.11022, found 289.11069.

4.1.40. Synthesis of 6-methoxy-1-(4-methoxybenzyl)-1,2,3,4-tetrahydroquinoxaline (7g)

Colorless oil (33.0%). HPLC purity: 95.97%, retention time: 8.48 min. ^{1}H NMR (300 MHz, $CDCl_3$) δ 7.24 (d, $J = 8.6$ Hz, 2H), 6.86 (d, $J = 8.6$ Hz, 2H), 6.51 (d, $J = 8.7$ Hz, 1H), 6.29–6.07 (m, 2H), 4.26 (s, 2H), 3.79 (s, 3H), 3.69 (s, 3H), 3.40 (s, 2H), 3.23 (s, 2H). ^{13}C NMR (75 MHz, $CDCl_3$) δ 158.67, 152.88, 135.63, 130.94, 129.86, 128.69, 113.98, 113.63, 102.92, 100.97, 55.82, 55.58, 55.34, 47.64, 41.16. HRMS (ESI) *m/z* calcd for $C_{17}H_{21}N_2O_2^+$ $[M+H]^+$ 285.15975, found 285.15967.

4.1.41. Synthesis of 6-methoxy-1-(3-methoxybenzyl)-1,2,3,4-tetrahydroquinoxaline (7h)

Colorless oil (32.1%). HPLC purity: 96.17%, retention time: 8.47 min. ^{1}H NMR (300 MHz, $CDCl_3$) δ 7.22 (d, $J = 7.7$ Hz, 1H), 6.94–6.87 (m, 2H), 6.79 (d, $J = 8.2$ Hz, 1H), 6.47 (d, $J = 8.8$ Hz, 1H), 6.29–6.02 (m, 2H), 4.30 (s, 2H), 3.78 (s, 3H), 3.69 (s, 3H), 3.41 (s, 2H), 3.25 (s, 2H). ^{13}C NMR (75 MHz, $CDCl_3$) δ 159.92, 152.81, 140.90, 140.84, 135.47, 129.58, 119.67, 113.47, 112.85, 112.26, 102.90, 100.95, 56.46, 55.57, 55.23, 48.02, 41.15. HRMS (ESI) *m/z* calcd for $C_{17}H_{21}N_2O_2^+$ $[M+H]^+$ 285.15975, found 285.15976.

4.1.42. Synthesis of 6-methoxy-1-((6-methoxynaphthalen-2-yl)methyl)-1,2,3,4-tetrahydroquinoxaline (7i)

White solid (48.7%). HPLC purity: 95.63%, retention time: 10.68 min. m.p.: 116–117 °C. ^{1}H NMR (300 MHz, $CDCl_3$) δ 7.74–7.67 (m, 3H), 7.43 (d, $J = 8.4$ Hz, 1H), 7.16–7.11 (m, 2H), 6.56 (d, $J = 8.7$ Hz, 1H), 6.35–6.03 (m, 2H), 4.45 (s, 2H), 3.92 (s, 3H), 3.71 (s, 3H), 3.45 (s, 2H), 3.28 (s, 2H). ^{13}C NMR (75 MHz, $CDCl_3$) δ 157.62, 153.07, 133.93, 129.32, 129.10, 127.26, 126.47, 125.97, 118.93, 105.89, 55.70, 55.46, 48.07, 41.24, 29.85. HRMS (ESI) *m/z* calcd for $C_{21}H_{23}N_2O_2^+$ $[M+H]^+$ 335.17540, found 335.17529.

4.1.43. Synthesis of 1-benzyl-6-ethoxy-1,2,3,4-tetrahydroquinoxaline (7j)

Colorless oil (25.5%). HPLC purity: 96.89%, retention time: 7.96 min. ^{1}H NMR (300 MHz, $CDCl_3$) δ 7.36–7.30 (m, 4H), 7.26–7.19 (m, 1H), 6.46 (d, $J = 8.8$ Hz, 1H), 6.24–6.09 (m, 2H), 4.33 (s, 2H), 3.90 (q, $J = 6.8$ Hz, 2H), 3.41 (s, 2H), 3.25 (s, 2H), 1.34 (t, $J = 7.0$ Hz, 3H). ^{13}C NMR (75 MHz, $CDCl_3$) δ 152.10, 139.13, 135.42, 129.78, 128.60, 127.41, 126.94, 113.49, 103.89, 101.74, 63.77, 56.43, 48.04, 41.18, 15.15. HRMS (ESI) *m/z* calcd for $C_{17}H_{21}N_2O^+$ $[M+H]^+$ 269.16539, found 269.16540.

4.1.44. Synthesis of 6-ethoxy-1-(3,4,5-trimethoxybenzyl)-1,2,3,4-tetrahydroquinoxaline (7k)

Colorless oil (63.8%). HPLC purity: 97.28%, retention time: 7.78 min. ^{1}H NMR (300 MHz, $CDCl_3$) δ 6.57 (s, 2H), 6.53 (d, $J = 8.7$ Hz, 1H), 6.34–6.10 (m, 2H), 4.25 (s, 2H), 4.01–3.88 (m, 2H), 3.84 (s, 3H), 3.83 (s, 6H), 3.43 (s, 2H), 3.22 (s, 2H), 1.35 (t, $J = 7.0$ Hz, 3H). ^{13}C NMR (75 MHz, $CDCl_3$) δ 153.42, 152.33, 136.80, 135.60, 134.91, 129.75, 113.85, 104.13, 103.95, 101.68, 63.78, 60.89, 56.88, 56.14, 47.77, 41.14, 15.06. HRMS (ESI) *m/z* calcd for $C_{20}H_{27}N_2O_4^+$ $[M+H]^+$ 359.19653, found 359.19681.

4.1.45. Synthesis of tert-butyl 4-benzyl-7-methoxy-3,4-dihydroquinoxaline-1(2H)-carboxylate (8)

To a solution of **7d** (1.00 g, 3.92 mmol) in DCM (25 mL) was added di-*tert*-butyl dicarbonate (1.72 g, 7.86 mmol) and TEA (0.80 g, 7.86 mmol), the mixture reaction was stirred at 40 °C for 15 h. Then the reaction was cooled to room temperature, washed with water and dried over anhydrous Na_2SO_4, filtered. The filtrate was concentrated and purified by chromatography (PE:EA = 20:1) to afford **8** (0.90 g, 71.8%) as a white solid. m.p.: 103–104 °C. ^{1}H NMR (300 MHz, $CDCl_3$) δ 7.38–7.26 (m, 4H), 7.25–7.15 (m, 2H), 6.60–6.51 (m, 2H), 4.45 (s, 2H), 3.83 (t, $J = 5.2$ Hz, 2H), 3.74 (s, 3H), 3.34 (t, $J = 5.1$ Hz, 2H), 1.54 (s, 9H). MS (ESI) $[M+H]^+$ 355.11.

4.1.46. Synthesis of tert-butyl 7-methoxy-3,4-dihydroquinoxaline-1(2H)-carboxylate (9)

10% Pd/C (0.13 g, 0.12 mmol) was added to the solution of **8** (0.90 g, 2.54 mmol) in methanol (40 mL) and the mixture was stirred at room temperature under H_2 atmosphere. After completion, the mixture was filtrated with Celite, and the filtrate was concentrated under vacuum and purified by chromatography (PE:EA = 9:1) to give **9** (0.58 g, 86.4%) as a white solid. m.p.: 70–72 °C. ^{1}H NMR (300 MHz, $CDCl_3$) δ 7.23 (s, 1H), 6.57–6.48 (m, 2H), 3.78 (t, $J = 5.0$ Hz, 2H), 3.74 (s, 3H), 3.36 (t, $J = 5.0$ Hz, 2H), 1.53 (s, 9H). MS (ESI) $[M+H]^+$ 264.11.

4.1.47. Synthesis of tert-butyl 7-methoxy-4-(3,4,5-trimethoxybenzoyl)-3,4-dihydroquinoxaline-1(2H)-carboxylate (10a)

To **9** (0.11 g, 0.42 mmol) and 4-dimethylaminopyridine (0.078 g, 0.64 mmol) in anhydrous DCM (5 mL) was added 3,4,5-trimethoxybenzoyl chloride (0.15 g, 0.64 mmol) in DCM (2 mL), and the mixture was stirred at room temperature for 3 h. After completion, the mixture was washed with 2 N HCl, water and dried over anhydrous Na_2SO_4, filtered. The filtrate was concentrated and purified by chromatography (PE:EA = 6:1) to afford **10a** (0.16 g, 85.2%) as a yellow oil. ^{1}H NMR (300 MHz, $CDCl_3$) δ 7.41 (s, 1H), 6.62 (s, 2H), 6.58 (d, $J = 9.4$ Hz, 1H), 6.39 (d, $J = 8.8$ Hz, 1H), 4.05 (t, $J = 6.3$ Hz, 2H), 3.93 (t, $J = 6.4$ Hz, 2H), 3.84 (s, 3H), 3.76 (s, 3H), 3.69 (s, 6H), 1.55 (s, 9H). MS (ESI) $[M+H]^+$ 459.13.

Compounds **10b**–**10l** were synthesized following a similar method of compound **10a**.

*4.1.48. Synthesis of tert-butyl 4-(3,5-dimethoxybenzoyl)-7-methoxy-3,4-dihydroquinoxaline-1(2H)-carboxylate **(10b)***

Colorless oil (73.6%). ^{1}H NMR (300 MHz, $CDCl_3$) δ 7.46 (s, 1H), 6.78–6.59 (m, 1H), 6.54–6.49 (m, 2H), 6.47–6.43 (m, 1H), 6.38 (d, J = 9.1 Hz, 1H), 4.01 (t, J = 5.5 Hz, 2H), 3.91 (t, J = 5.5 Hz, 2H), 3.76 (s, 3H), 3.69 (s, 6H), 1.56 (s, 9H). MS (ESI) $[M+H]^+$ 429.19.

*4.1.49. Synthesis of tert-butyl 4-(4-chloro-3-nitrobenzoyl)-7-methoxy-3,4-dihydroquinoxaline-1(2H)-carboxylate **(10c)***

Yellow solid (86.4%). m.p.: 61–64 °C. ^{1}H NMR (300 MHz, $CDCl_3$) δ 8.02 (s, 1H), 7.55 (s, 1H), 7.45–7.38 (m, 2H), 6.50–6.31 (m, 2H), 4.06 (t, J = 6.2 Hz, 2H), 3.94 (t, J = 6.1 Hz, 2H), 3.77 (s, 3H), 1.58 (s, 9H). MS (ESI) $[M+H]^+$ 448.94.

*4.1.50. Synthesis of tert-butyl 4-(benzo[d][1,3]dioxole-5-carbonyl)-7-methoxy-3,4-dihydroquinoxaline-1(2H)-carboxylate **(10d)***

Yellow oil (69.8%). ^{1}H NMR (300 MHz, $CDCl_3$) δ 7.58–7.48 (m, 1H), 6.96–6.90 (m, 2H), 6.69 (d, J = 8.4 Hz, 1H), 6.55 (d, J = 8.9 Hz, 1H), 6.37 (dd, J = 8.9, 2.7 Hz, 1H), 5.97 (s, 2H), 3.99 (d, J = 6.0 Hz, 2H), 3.90 (t, J = 5.8 Hz, 2H), 3.77 (s, 3H), 1.57 (s, 9H). MS (ESI) $[M+H]^+$ 413.19.

*4.1.51. Synthesis of tert-butyl 4-(2,3-dichloro-1-methyl-1H-indole-5-carbonyl)-7-methoxy-3,4-dihydroquinoxaline-1(2H)-carboxylate **(10e)***

White solid (78.6%). m.p.: 173–174 °C. ^{1}H NMR (300 MHz, $CDCl_3$) δ 7.80 (s, 1H), 7.53 (s, 1H), 7.20 (d, J = 7.1 Hz, 1H), 7.10 (d, J = 8.5 Hz, 1H), 6.49 (d, J = 8.2 Hz, 1H), 6.27 (d, J = 9.0 Hz, 1H), 4.06 (t, J = 6.1 Hz, 2H), 3.94 (t, J = 6.3 Hz, 2H), 3.74 (s, 3H), 3.73 (s, 3H), 1.59 (s, 9H). MS (ESI) $[M+H]^+$ 455.99.

*4.1.52. Synthesis of tert-butyl 7-methoxy-4-(6-methoxy-2-naphthoyl)-3,4-dihydroquinoxaline-1(2H)-carboxylate **(10f)***

Colorless oil (79.0%). ^{1}H NMR (300 MHz, $CDCl_3$) δ 7.99 (s, 1H), 7.72 (d, J = 9.0 Hz, 1H), 7.62–7.54 (m, 2H), 7.34 (d, J = 8.4 Hz, 1H), 7.15 (dd, J = 8.9, 2.4 Hz, 1H), 7.11–7.06 (m, 1H), 6.52 (d, J = 4.7 Hz, 1H), 6.25 (dd, J = 9.3, 2.7 Hz, 1H), 4.08 (t, J = 6.3 Hz, 2H), 3.96 (t, J = 6.1 Hz, 2H), 3.91 (s, 3H), 3.74 (s, 3H), 1.60 (s, 9H). MS (ESI) $[M+H]^+$ 450.18.

*4.1.53. Synthesis of tert-butyl 7-methoxy-4-(quinoline-6-carbonyl)-3,4-dihydroquinoxaline-1(2H)-carboxylate **(10g)***

Colorless oil (72.0%). ^{1}H NMR (300 MHz, $CDCl_3$) δ 8.45–8.29 (m, 3H), 8.20–8.07 (m, 2H), 8.05–8.00 (m, 1H),7.99 (d, J = 8.7 Hz, 1H), 7.70 (dd, J = 7.9, 3.4 Hz, 1H), 7.48 (d, J = 7.4 Hz, 1H), 4.07 (t, J = 6.2 Hz, 2H), 3.97 (t, J = 6.2 Hz, 2H), 3.85 (s, 3H), 1.62 (s, 9H).

*4.1.54. Synthesis of tert-butyl 7-methoxy-4-(quinoline-5-carbonyl)-3,4-dihydroquinoxaline-1(2H)-carboxylate **(10h)***

Yellow oil (72.3%). ^{1}H NMR (300 MHz, $CDCl_3$) δ 8.95 (dd, J = 4.1, 1.6 Hz, 1H), 8.15 (d, J = 8.2 Hz, 1H), 8.02 (d, J = 1.6 Hz, 1H), 7.98 (d, J = 8.8 Hz, 1H), 7.62 (dd, J = 8.8, 1.6 Hz, 1H), 7.60–7.56 (m, 1H), 7.43 (dd, J = 8.3, 4.2 Hz, 1H), 6.59–6.33 (m, 1H), 6.24 (dd, J = 8.9, 2.1 Hz, 1H), 4.10 (t, J = 6.2 Hz, 2H), 3.97 (t, J = 6.2 Hz, 2H), 3.74 (s, 3H), 1.60 (s, 9H). MS (ESI) $[M+H]^+$ 420.12.

*4.1.55. Synthesis of tert-butyl 7-methoxy-4-(2-oxo-2H-chromene-3-carbonyl)-3,4-dihydroquinoxaline-1(2H)-carboxylate **(10i)***

Yellow solid (75.7%). m.p.: 94–95 °C. ^{1}H NMR (300 MHz, $CDCl_3$) δ 7.87 (s, 1H), 7.64–7.47 (m, 3H), 7.34–7.25 (m, 2H), 6.73 (s, 1H), 6.35 (s, 1H), 4.03 (s, 2H), 3.94 (s, 2H), 3.74 (s, 3H), 1.57 (s, 9H). MS (ESI) $[M+H]^+$ 437.12.

*4.1.56. Synthesis of tert-butyl 4-(6-bromo-2-oxo-2H-chromene-3-carbonyl)-7-methoxy-3,4-dihydroquinoxaline-1(2H)-carboxylate **(10j)***

Yellow solid (82.5%). m.p.: 198–199 °C. ^{1}H NMR (300 MHz, $CDCl_3$) δ 7.78 (s, 1H), 7.70–7.57 (m, 3H), 7.23–7.12 (m, 1H), 6.77–6.63 (m, 1H), 6.42–6.26 (m, 1H), 4.11–3.97 (m, 2H), 3.97–3.88 (m, 2H), 3.75 (s, 3H), 1.57 (s, 9H). MS (ESI) $[M+H]^+$ 516.24.

*4.1.57. Synthesis of tert-butyl 4-(cyclohexanecarbonyl)-7-methoxy-3,4-dihydroquinoxaline-1(2H)-carboxylate **(10k)***

White solid (87.3%). m.p.: 80–81 °C. ^{1}H NMR (300 MHz, $CDCl_3$) δ 6.91 (d, J = 8.0 Hz, 1H), 6.26–6.19 (m, 2H), 3.90 (t, J = 5.2 Hz, 2H), 3.71 (s, 3H), 3.39 (t, J = 5.2 Hz, 2H), 2.93 (t, J = 11.0 Hz, 1H), 1.93–1.44 (m, 10*H*), 1.56 (s, 9H). MS (ESI) $[M+H]^+$ 375.22.

*4.1.58. Synthesis of tert-butyl 4-(adamantane-1-carbonyl)-7-methoxy-3,4-dihydroquinoxaline-1(2H)-carboxylate **(10l)***

White solid (89.5%). m.p.: 143–145 °C. ^{1}H NMR (300 MHz, $CDCl_3$) δ 7.18–7.13 (m, 1H), 6.23–6.18 (m, 2H), 3.98 (t, J = 5.3 Hz, 2H), 3.70 (s, 3H), 3.41 (t, J = 5.4 Hz, 2H), 2.06–1.96 (m, 11*H*), 1.94–1.91 (m, 1H), 1.75–1.70 (m, 2H), 1.65–1.60 (m, 1H), 1.57 (s, 9H). MS (ESI) $[M+H]^+$ 427.27.

*4.1.59. Synthesis of (6-methoxy-3,4-dihydroquinoxalin-1(2H)-yl)(3,4,5-trimethoxyphenyl)methanone **(11a)***

To a solution of **10a** (0.060 g, 0.14 mmol) in DCM (5 mL) was added trifluoroacetic acid (51 μL, 0.69 mmol), and the mixture was stirred overnight at room temperature. After completion, the mixture was washed with water and brine, and then dried over Na_2SO_4, filtered. The filtrate was concentrated and purified by chromatography (PE:EA = 6:1) to afford **11a** (0.044 g, 89.8%) as a white solid. HPLC purity: 95.80%, retention time: 6.97 min. m.p.: 115–117 °C. ^{1}H NMR (300 MHz, $CDCl_3$) δ 6.68 (s, 2H), 6.65–6.24 (m, 1H), 6.14 (d, J = 2.7 Hz, 1H), 6.02 (d, J = 8.9 Hz, 1H), 3.96 (t, J = 5.2 Hz, 2H), 3.85 (s, 3H), 3.74 (s, 6H), 3.71 (s, 3H), 3.54 (t, J = 5.2 Hz, 2H). ^{13}C NMR (75 MHz, $CDCl_3$) δ 157.83, 152.79, 139.61, 137.92, 130.71, 125.93, 118.49, 106.34, 102.31, 100.10, 99.38, 60.93, 56.22, 56.15, 55.32, 42.72. HRMS (ESI) *m/z* calcd for $C_{19}H_{23}N_2O_5^+$ $[M+H]^+$ 359.16015, found 359.16052.

Compounds **11b**–**11l** were synthesized following a similar method of compound **11a**.

*4.1.60. Synthesis of (3,5-dimethoxyphenyl)(6-methoxy-3,4-dihydroquinoxalin-1(2H)-yl)methanone **(11b)***

Brown oil (77.4%). HPLC purity: 96.65%, retention time: 7.15 min. ^{1}H NMR (300 MHz, $CDCl_3$) δ 6.57 (d, J = 2.3 Hz, 2H), 6.46 (t, J = 1.7 Hz, 1H), 6.12 (d, J = 2.6 Hz, 1H), 6.03 (s, 1H), 3.92 (d, J = 3.0 Hz, 2H), 3.72 (s, 6H), 3.70 (s, 3H), 3.51 (s, 1H), 3.49 (d, J = 3.0 Hz, 2H). ^{13}C NMR (75 MHz, $CDCl_3$) δ 160.61, 157.87, 138.04, 137.96, 125.88, 118.31, 118.20, 106.41, 102.55, 102.46, 99.45, 55.57, 55.37, 42.76, 29.80. HRMS (ESI) *m/z* calcd for $C_{18}H_{21}N_2O_4^+$ $[M+H]^+$ 329.14958, found 329.14984.

*4.1.61. Synthesis of (4-chloro-3-nitrophenyl)(6-methoxy-3,4-dihydroquinoxalin-1(2H)-yl)methanone **(11c)***

Yellow solid (78.3%). HPLC purity: 97.45%, retention time: 8.32 min. m.p.: 71–73 °C. ^{1}H NMR (300 MHz, $CDCl_3$) δ 7.99 (d, J = 1.9 Hz, 1H), 7.52 (d, J = 8.3 Hz, 1H), 7.46 (d, J = 8.3 Hz, 1H), 6.65–6.17 (m, 1H), 6.15 (d, J = 2.6 Hz, 1H), 6.03–5.89 (m, 1H), 3.97 (t, J = 5.7 Hz, 2H), 3.71 (s, 3H), 3.58 (t, J = 5.4 Hz, 2H). ^{13}C NMR (75 MHz, $CDCl_3$) δ 164.41, 158.50, 147.54, 138.28, 135.82, 133.23, 131.51, 128.55, 126.31, 125.87, 117.23, 102.53, 99.60, 55.30, 42.63, 29.70. HRMS (ESI) *m/z* calcd for $C_{16}H_{15}ClN_3O_4^+$ $[M+H]^+$ 348.07456, found 348.07483.

*4.1.62. Synthesis of benzo[d][1,3]dioxol-5-yl(6-methoxy-3,4-dihydroquinoxalin-1(2H)-yl)methanone **(11d)***

White oil (74.6%). HPLC purity: 96.32%, retention time: 7.20 min. ^{1}H NMR (300 MHz, $CDCl_3$) δ 6.98 (dd, J = 8.0, 1.6 Hz, 1H), 6.95 (d, J = 1.4 Hz, 1H), 6.72 (d, J = 8.0 Hz, 1H), 6.69–6.31 (m, 1H), 6.12 (d, J = 2.7 Hz, 1H), 6.01 (dd, J = 8.9, 2.3 Hz, 1H), 5.97 (s, 2H), 3.93 (t, J = 5.2 Hz, 2H), 3.70 (s, 3H), 3.51 (t, J = 5.2 Hz, 2H). ^{13}C NMR (75 MHz, $CDCl_3$) δ 167.99, 157.80, 149.22, 147.41, 137.93, 129.79, 125.98, 123.85, 118.81, 109.51, 108.01, 102.67, 101.51, 99.47, 55.37, 42.92, 41.37.

HRMS (ESI) *m/z* calcd for $C_{17}H_{17}N_2O_4^+$ $[M+H]^+$ 313.11828, found 313.11859.

*4.1.63. Synthesis of (2,3-dichloro-1-methyl-1H-indol-5-yl)(6-methoxy-3,4-dihydroquinoxalin-1(2H)-yl)methanone **(11e)***

Yellow solid (72.6%). HPLC purity: 98.10%, retention time: 9.53 min. m.p.: 157–158 °C. ^{1}H NMR (300 MHz, $CDCl_3$) δ 7.78 (s, 1H), 7.29 (d, J = 8.2 Hz, 1H), 7.14 (d, J = 8.6 Hz, 1H), 6.79–6.23 (m, 1H), 6.14 (d, J = 2.7 Hz, 1H), 5.91 (d, J = 8.9 Hz, 1H), 3.98 (t, J = 5.2 Hz, 2H), 3.73 (s, 3H), 3.68 (s, 3H), 3.54 (t, J = 5.2 Hz, 2H). ^{13}C NMR (75 MHz, $CDCl_3$) δ 169.08, 157.69, 138.00, 135.30, 128.74, 126.10, 124.23, 124.09, 123.84, 119.41, 119.01, 108.97, 103.40, 102.57, 99.48, 55.38, 42.95, 30.69, 29.83. HRMS (ESI) *m/z* calcd for $C_{19}H_{18}Cl_2N_3O_2^+$ $[M+H]^+$ 390.07706, found 390.07745.

*4.1.64. Synthesis of (6-methoxy-3,4-dihydroquinoxalin-1(2H)-yl)(6-methoxynaph-thalen-2-yl)methanone **(11f)***

Yellow solid (78.3%). HPLC purity: 95.90%, retention time: 8.22 min. m.p.: 109–110 °C. ^{1}H NMR (300 MHz, $CDCl_3$) δ 7.98 (s, 1H), 7.72 (d, J = 8.9 Hz, 1H), 7.62 (d, J = 8.5 Hz, 1H), 7.42 (d, J = 8.6 Hz, 1H), 7.15 (dd, J = 8.8, 2.4 Hz, 1H), 7.12–7.07 (m, 1H), 6.55 (s, 1H), 6.15 (d, J = 2.7 Hz, 1H), 5.91 (d, J = 9.0 Hz, 1H), 4.12 (s, 1H), 4.01 (t, J = 5.2 Hz, 2H), 3.92 (s, 3H), 3.68 (s, 3H), 3.57 (t, J = 5.2 Hz, 2H). ^{13}C NMR (75 MHz, $CDCl_3$) δ 168.75, 158.93, 157.80, 138.03, 135.50, 131.21, 130.40, 129.27, 128.23, 126.44, 126.34, 126.16, 119.47, 118.90, 105.81, 102.55, 99.58, 55.49, 55.37, 42.99, 29.85. HRMS (ESI) *m/z* calcd for $C_{21}H_{21}N_2O_3^+$ $[M+H]^+$ 349.15467, found 349.15494.

*4.1.65. Synthesis of (6-methoxy-3,4-dihydroquinoxalin-1(2H)-yl) (quinolin-8-yl) methanone **(11g)***

Yellow solid (75.4%). HPLC purity: 97.00%, retention time: 6.78 min. m.p.: 105–106 °C. ^{1}H NMR (300 MHz, $CDCl_3$) δ 9.02–8.91 (m, 1H), 8.16 (d, J = 8.0 Hz, 1H), 8.05 (s, 1H), 8.00 (d, J = 8.5 Hz, 1H), 7.67 (d, J = 8.3 Hz, 1H), 7.43 (dd, J = 8.3, 4.2 Hz, 1H), 6.73–6.09 (m, 2H), 6.01–5.67 (m, 1H), 4.03 (s, 2H), 3.67 (s, 3H), 3.60 (s, 2H). ^{13}C NMR (75 MHz, $CDCl_3$) δ 157.93, 151.65, 148.50, 138.05, 136.83, 134.28, 129.23, 129.20, 129.12, 129.09, 128.98, 127.69, 126.04, 121.72, 102.30, 99.48, 55.25, 42.78, 28.42. HRMS (ESI) *m/z* calcd for $C_{19}H_{18}N_3O_2^+$ $[M+H]^+$ 320.13935, found 320.13983.

*4.1.66. Synthesis of (6-methoxy-3,4-dihydroquinoxalin-1(2H)-yl) (quinolin-6-yl) methanone **(11h)***

Yellow solid (71.5%). HPLC purity: 97.17%, retention time: 6.69 min. m.p.: 104–105 °C. ^{1}H NMR (300 MHz, $CDCl_3$) δ 8.95 (d, J = 2.7 Hz, 1H), 8.17 (d, J = 8.2 Hz, 1H), 8.05 (s, 1H), 8.01 (d, J = 8.6 Hz, 1H), 7.68 (d, J = 8.5 Hz, 1H), 7.44 (dd, J = 8.2, 4.2 Hz, 1H), 7.05–6.26 (m, 1H), 6.15 (d, J = 2.7 Hz, 1H), 5.86 (d, J = 8.9 Hz, 1H), 4.02 (t, J = 5.2 Hz, 2H), 3.67 (s, 3H), 3.59 (t, J = 5.2 Hz, 2H). ^{13}C NMR (75 MHz, $CDCl_3$) δ 158.07, 151.60, 148.42, 138.20, 137.09, 134.48, 129.39, 129.15, 129.06, 127.81, 126.13, 121.82, 118.26, 102.45, 99.63, 55.35, 42.89, 29.83. HRMS (ESI) *m/z* calcd for $C_{19}H_{18}N_3O_2^+$ $[M+H]^+$ 320.13935, found 320.13977.

*4.1.67. Synthesis of 3-(6-methoxy-1,2,3,4-tetrahydroquinoxaline-1-carbonyl)–2H-chromen-2-one **(11i)***

Yellow solid (68.3%). HPLC purity: 96.61%, retention time: 6.81 min. m.p.: 131–133 °C. ^{1}H NMR (300 MHz, $CDCl_3$) δ 8.00 (s, 1H), 7.54 (d, J = 7.6 Hz, 2H), 7.32 (d, J = 8.2 Hz, 2H), 6.57 (d, J = 9.3 Hz, 1H), 6.13 (s, 1H), 5.91 (d, J = 8.1 Hz, 1H), 3.76 (s, 2H), 3.67 (s, 3H), 3.61 (s, 2H). ^{13}C NMR (75 MHz, $CDCl_3$) δ 163.46, 158.55, 157.17, 154.16, 143.54, 139.00, 132.60, 128.59, 126.40, 124.72, 123.80, 118.29, 117.59, 116.81, 102.01, 99.38, 55.15, 42.18, 40.01. HRMS (ESI) *m/z* calcd for $C_{19}H_{17}N_2O_4^+$ $[M+H]^+$ 337.11828, found 337.11847.

*4.1.68. Synthesis of 6-bromo-3-(6-methoxy-1,2,3,4-tetrahydroquinoxaline-1-carbonyl)–2H-chromen-2-one **(11j)***

Yellow solid (79.8%). HPLC purity: 97.68%, retention time: 7.73 min. m.p.: 185–187 °C. ^{1}H NMR (300 MHz, $CDCl_3$) δ 7.90 (s, 1H), 7.67–7.59 (m, 2H), 7.17 (d, J = 8.6 Hz, 1H), 6.53 (d, J = 8.6 Hz, 1H), 6.12 (s, 1H), 5.90 (d, J = 8.3 Hz, 1H), 3.66 (s, 3H), 3.59 (s, 2H), 3.48 (s, 2H). ^{13}C NMR (75 MHz, $CDCl_3$) δ 162.95, 158.70, 156.48, 152.97, 142.02, 139.01, 135.27, 130.69, 127.60, 123.82, 119.79, 118.57, 117.29, 102.09, 99.41, 55.17, 50.91, 42.16, 40.04. HRMS (ESI) *m/z* calcd for $C_{19}H_{16}BrN_2O_4^+$ $[M+H]^+$ 415.02880, found 415.02899.

*4.1.69. Synthesis of cyclohexyl(6-methoxy-3,4-dihydroquinoxalin-1(2H)-yl) methanone **(11k)***

White solid (63.6%). HPLC purity: 98.63%, retention time: 8.64 min. m.p.: 104–105 °C. ^{1}H NMR (300 MHz, $CDCl_3$) δ 6.89–6.75 (m, 1H), 6.15 (dd, J = 8.7, 2.7 Hz, 1H), 6.07 (d, J = 2.4 Hz, 1H), 4.10 (br, 1H), 3.71 (t, J = 5.0 Hz, 2H), 3.68 (s, 3H), 3.38–3.25 (m, 2H), 2.94–2.78 (m, 1H), 1.71–1.61 (m, 4H), 1.59–1.39 (m, 4H), 1.17–1.10 (m, 2H). ^{13}C NMR (75 MHz, $CDCl_3$) δ 176.09, 158.35, 139.12, 125.07, 118.38, 102.10, 99.33, 55.32, 42.79, 40.67, 39.07, 29.71, 25.80, 25.66. HRMS (ESI) *m/z* calcd for $C_{16}H_{23}N_2O_2^+$ $[M+H]^+$ 275.17595, found 275.17618.

*4.1.70. Synthesis of (adamantan-1-yl)(6-methoxy-3,4-dihydroquinoxalin-1(2H)-yl)methanone **(11l)***

White solid (76.4%). HPLC purity: 98.13%, retention time: 10.35 min. m.p.: 173–174 °C. ^{1}H NMR (300 MHz, $CDCl_3$) δ 7.18 (d, J = 8.8 Hz, 1H), 6.21 (dd, J = 8.8, 2.7 Hz, 1H), 6.09 (d, J = 2.6 Hz, 1H), 4.00 (br, 1H), 3.90 (t, J = 5.0 Hz, 2H), 3.73 (s, 3H), 3.42 (t, J = 5.0 Hz, 2H), 2.06–1.98 (m, 9H), 1.75–1.67 (m, 6H). ^{13}C NMR (75 MHz, $CDCl_3$) δ 176.84, 157.97, 139.03, 127.02, 119.91, 102.22, 99.40, 55.32, 43.70, 43.41, 43.19, 39.45, 36.63, 28.55. HRMS (ESI) *m/z* calcd for $C_{20}H_{27}N_2O_2^+$ $[M+H]^+$ 327.20725, found 327.20737.

4.2. Biological evaluations

4.2.1. Cell culture

Hela cells (human epithelial cervical cancer cell line) and HT-29 cells (human intestinal epithelial cell line) were both obtained from the American Type Culture Collection (ATCC, USA). Cultures were maintained in RPMI 1640 medium (HyClone Co., USA) containing with 10% (v/v) fetal bovine serum (Sijiqing Biotechnology Co., China) under a humidified atmosphere containing 5% (v/v) CO_2 at 37 °C.

4.2.2. Cell proliferation inhibitory assay

Cells were seeded in 96-well plates at a concentration of 4.5×10^3 cells per well, which were incubated at 37 °C, 5% CO_2 for 24 h. After incubation, the cells were treated with the tested compounds or positive controls at different concentrations and incubated for further 72 h. Then 50 μL of MTT reagent was added per well, incubated at 37 °C for 4 h. After incubation, MTT solution was discarded, and 100 μL DMSO was added to dissolve the MTT formazan completely. The OD (optical density) was measured at a wavelength of 570 nm using a microplate reader. The inhibition rate (%) = $(OD_{control} - OD_{compound}) / (OD_{control} - OD_{blank}) \times 100\%$. IC_{50} values were calculated with normalized dose-response using Origin software.

4.2.3. Tubulin polymerization inhibitory assay

Tubulin polymerization inhibitory assay was conducted using the Tubulin Polymerization Assay Kit (BK011P, Cytoskeleton, USA) according to the manufacturer. Compound **11a** at various concentrations and the positive control colchicine were added to 96-well plates and incubated at 37 °C for 1 min. Then the tubulin reagent (2.0 mg/mL porcine brain tubulin in 80 mM PIPES pH 6.9, 2.0 mM $MgCl_2$, 0.5 mM EGTA, 1.0 mM GTP and 15% glycerol) was added per well and mixed. The mixture was monitored (excitation: 360 nm, emission: 450 nm) every 60 s for 80 min using a multifunction microplate reader.

4.2.4. Immunofluorescence analysis

Hela cells were seeded into 96-well plates, which were incubated at 37 °C, 5% CO_2 for 24 h. Then compound **11a** at various concentrations were added and incubated for further 24 h. After fixed in 3.7% paraformaldehyde in the dark at 25 °C for 5 min, Hela cells were permeabilized with 0.1% Triton X-100 for 5 min and blocked with 1% BSA for 1 h at 25 °C. Then these cells were incubated with the primary antibody (1:100 dilution in 1% BSA-PBS) overnight at 4 °C. After incubation, these cells were washed with PBS and incubated with the secondary antibody labeled with Cy3 (1:100 dilution in 1% BSA-PBS) at 25 °C for 2 h in the dark. Finally, these cells were washed with PBS three times, and the nuclei were stained with Hoechst 33,342 at room temperature for 25 min. The immunofluorescence was observed using a fluorescence microscope.

4.2.5. Cell cycle analysis

Hela cells were seeded in 6-well plates, which were incubated at 37 °C, 5% CO_2 for 24 h. After incubation, the cells were treated with compound **11a** at various concentrations and incubated for further 24 h. Then the cells were harvested by centrifugation and fixed in ice-cold 70% ethanol at −20 °C for 48 h. After washing, the cells were stained with 500 μL of dye (50 μg/mL of PI and 100 μg/mL of RNasaA) in the dark for 1 h at 4 °C. The cells were analyzed by flow cytometry using FACS Calibur instrument.

4.2.6. Apoptosis analysis

Hela cells were seeded in 6-well plates, which were incubated at 37 °C, 5% CO_2 for 24 h. Cells were treated with compound **11a** at various concentrations for 24 h, then harvested. Subsequently, the cells were stained with 500 μL of dye (50 μg/mL of PI and 100 μg/mL of FITC AV) at room temperature for 30 min in the dark. The cells were detected by flow cytometry.

4.2.7. Cytotoxicity assay

The experiment procedure was similar with the cell proliferation inhibitory assay.

4.2.8. Molecular docking

Molecular docking study was performed using Maestro 11.5 and the X-ray crystal structure of tubulin-combretastatin A4 (PDB: 5LYJ) was retrieved from RCSB Protein Data Bank. The protein was prepared using Protein Preparation Wizard to add hydrogen, remove water, fill in missing side/loops and minimize energy. Subsequently, Grid was generated by receptor grid generation, following the standard procedure recommended by Schrodinger. Then compound **11a** was prepared by adding hydrogen atoms, generating 3D geometries and ionization, optimizing with OPLS3 force field. Compound **11a** was docked into the colchicine binding site using Glide with the standard precision mode (RMSD = 0.647 Å). Additionally, the figure was made using PyMOL.

Declaration of Competing Interest

The authors declare no competing financial interest.

Acknowledgements

This work was financially supported by National Natural Science Foundation of China (No. 81903443), Key-Scientific and Technological Project of Henan Province (No. 192102310146, No. 212102310316) and Key Scientific Research Program of the Higher Education Institutions of Henan Province (No. 20A310003).

Appendix A. Supplementary material

Supplementary data to this article can be found online at https://doi.org/10.1016/j.bioorg.2021.104793.

References

[1] R.A. Stanton, K.M. Gernert, J.H. Nettles, R. Aneja, Drugs that target dynamic microtubules: a new molecular perspective, Med. Res. Rev. 31 (2011) 443–481.
[2] F. Pellegrini, D.R. Budman, Review: tubulin function, action of antitubulin drugs, and new drug development, Cancer Invest. 23 (2005) 264–273.
[3] M. Dogterom, G.H. Koenderink, Actin-microtubule crosstalk in cell biology, Nat. Rev. Mol. Cell Biol. 20 (2019) 38–54.
[4] A. Akhmanova, M.O. Steinmetz, Control of microtubule organization and dynamics: two ends in the limelight, Nat. Rev. Mol. Cell Biol. 16 (2015) 711–726.
[5] D.A. Fletcher, R.D. Mullins, Cell mechanics and the cytoskeleton, Nature 463 (2010) 485–492.
[6] M. Borowiak, W. Nahaboo, M. Reynders, K. Nekolla, P. Jalinot, J. Hasserodt, M. Rehberg, M. Delattre, S. Zahler, A. Vollmar, D. Trauner, O. Thorn-Seshold, Photoswitchable Inhibitors of Microtubule Dynamics Optically Control Mitosis and Cell Death, Cell 162 (2015) 403–411.
[7] A. Fong, A. Durkin, H. Lee, The Potential of Combining Tubulin-Targeting Anticancer Therapeutics and Immune Therapy, Int. J. Mol. Sci. 20 (2019) 586–599.
[8] J. Seligmann, C. Twelves, Tubulin: an example of targeted chemotherapy, Future Med. Chem. 5 (2013) 339–352.
[9] J. Zich, K.G. Hardwick, Getting down to the phosphorylated 'nuts and bolts' of spindle checkpoint signalling, Trends Biochem. Sci. 35 (2010) 18–27.
[10] J.J. Field, A. Kanakkanthara, J.H. Miller, Microtubule-targeting agents are clinically successful due to both mitotic and interphase impairment of microtubule function, Bioorg. Med. Chem. 22 (2014) 5050–5059.
[11] E.C. McLoughlin, N.M. O'Boyle, Colchicine-Binding Site Inhibitors from Chemistry to Clinic: A Review, Pharmaceuticals (Basel) 13 (2020) 8–50.
[12] J.C.M. Meiring, B.I. Shneyer, A. Akhmanova, Generation and regulation of microtubule network asymmetry to drive cell polarity, Curr. Opin. Cell Biol. 62 (2020) 86–95.
[13] M. Tagliamento, C. Genova, G. Rossi, S. Coco, E. Rijavec, M.G. Dal Bello, S. Boccardo, F. Grossi, A. Alama, Microtubule-targeting agents in the treatment of non-small cell lung cancer: insights on new combination strategies and investigational compounds, Expert Opin. Investig. Drugs. 28 (2019) 513–523.
[14] N.G. Vindya, N. Sharma, M. Yadav, K.R. Ethiraj, Tubulins - The Target for Anticancer Therapy, Curr. Top Med. Chem. 15 (2015) 73–82.
[15] G. Chandrasekaran, P. Tatrai, F. Gergely, Hitting the brakes: targeting microtubule motors in cancer, Br. J. Cancer 113 (2015) 693–698.
[16] K. Haider, S. Rahaman, M.S. Yar, A. Kamal, Tubulin inhibitors as novel anticancer agents: an overview on patents (2013–2018), Expert Opin. Ther. Pat. 29 (2019) 623–641.
[17] H. Guo, X. Li, Y. Guo, L. Zhen, An overview of tubulin modulators deposited in protein data bank, Med. Chem. Res. 28 (2019) 927–937.
[18] Y. Izumi, S. Takagi, Vascular disrupting effect of combretastatin A-4 phosphate with inhibition of vascular endothelial cadherin in canine osteosarcoma-xenografted mice, Res. Vet. Sci. 122 (2019) 1–6.
[19] D. Bates, A. Eastman, Microtubule destabilising agents: far more than just antimitotic anticancer drugs, Br. J. Clin. Pharmacol. 83 (2017) 255–268.
[20] K.E. Arnst, Y. Wang, D.J. Hwang, Y. Xue, T. Costello, D. Hamilton, Q. Chen, J. Yang, F. Park, J.T. Dalton, D.D. Miller, W. Li, A. Potent, Metabolically Stable Tubulin Inhibitor Targets the Colchicine Binding Site and Overcomes Taxane Resistance, Cancer Res. 78 (2018) 265–277.
[21] Z. Wang, J. Chen, J. Wang, S. Ahn, C.M. Li, Y. Lu, V.S. Loveless, J.T. Dalton, D. D. Miller, W. Li, Novel tubulin polymerization inhibitors overcome multidrug resistance and reduce melanoma lung metastasis, Pharm. Res. 29 (2012) 3040–3052.
[22] Y. Finkelstein, S.E. Aks, J.R. Hutson, D.N. Juurlink, P. Nguyen, G. Dubnov-Raz, U. Pollak, G. Koren, Y. Bentur, Colchicine poisoning: the dark side of an ancient drug, Clinical toxicology (Philadelphia, Pa.) 48 (2010) 407–414.
[23] G.R. Pettit, M.R. Rhodes, D.L. Herald, E. Hamel, J.M. Schmidt, R.K. Pettit, Antineoplastic agents. 445. Synthesis and evaluation of structural modifications of (Z)- and (E)-combretastatin A-41, J. Med. Chem. 48 (2005) 4087–4099.
[24] K. Nepali, S. Sharma, M. Sharma, P.M. Bedi, K.L. Dhar, Rational approaches, design strategies, structure activity relationship and mechanistic insights for anticancer hybrids, Eur. J. Med. Chem. 77 (2014) 422–487.
[25] C.J. Maguire, Z. Chen, V.P. Mocharla, M. Sriram, T.E. Strecker, E. Hamel, H. Zhou, R. Lopez, Y. Wang, R.P. Mason, D.J. Chaplin, M.L. Trawick, K.G. Pinney, Synthesis of dihydronaphthalene analogues inspired by combretastatin A-4 and their biological evaluation as anticancer agents, Medchemcomm 9 (2018) 1649–1662.
[26] X. Wang, E. Wu, J. Wu, T.L. Wang, H.P. Hsieh, X. Liu, An antimitotic and antivascular agent BPR0L075 overcomes multidrug resistance and induces mitotic catastrophe in paclitaxel-resistant ovarian cancer cells, PLoS ONE 8 (2013) e65686.
[27] M.D. Canela, S. Noppen, O. Bueno, A.E. Prota, K. Bargsten, G. Saez-Calvo, M. L. Jimeno, M. Benkheil, D. Ribatti, S. Velazquez, M.J. Camarasa, J.F. Diaz, M. O. Steinmetz, E.M. Priego, M.J. Perez-Perez, S. Liekens, Antivascular and antitumor properties of the tubulin-binding chalcone TUB091, Oncotarget 8 (2017) 14325–14342.
[28] O. Bueno, G. Tobajas, E. Quesada, J. Estevez-Gallego, S. Noppen, M.J. Camarasa, J. F. Diaz, S. Liekens, E.M. Priego, M.J. Perez-Perez, Conformational mimetics of the alpha-methyl chalcone TUB091 binding tubulin: Design, synthesis and antiproliferative activity, Eur. J. Med. Chem. 148 (2018) 337–348.

[29] P. Oliva, R. Romagnoli, S. Manfredini, A. Brancale, S. Ferla, E. Hamel, R. Ronca, F. Maccarinelli, A. Giacomini, F. Rruga, E. Mariotto, G. Viola, R. Bortolozzi, Design, synthesis, in vitro and in vivo biological evaluation of 2-amino-3-aroylbenzo b furan derivatives as highly potent tubulin polymerization inhibitors, Eur. J. Med. Chem. 200 (2020) 112448–112464.

[30] I.K. Lindamulage, H.Y. Vu, C. Karthikeyan, J. Knockleby, Y.F. Lee, P. Trivedi, H. Lee, Novel quinolone chalcones targeting colchicine-binding pocket kill multidrug-resistant cancer cells by inhibiting tubulin activity and MRP1 function, Sci. Rep. 7 (2017) 10298–10310.

[31] J. Qi, H. Dong, J. Huang, S. Zhang, L. Niu, Y. Zhang, J. Wang, Synthesis and biological evaluation of N-substituted 3-oxo-1,2,3,4-tetrahydro-quinoxaline-6-carboxylic acid derivatives as tubulin polymerization inhibitors, Eur. J. Med. Chem. 143 (2018) 8–20.

[32] J. Qi, J. Huang, X. Zhou, W. Luo, J. Xie, L. Niu, Z. Yan, Y. Luo, Y. Men, Y. Chen, Y. Zhang, J. Wang, Synthesis and biological evaluation of quinoxaline derivatives as tubulin polymerization inhibitors that elevate intracellular ROS and triggers apoptosis via mitochondrial pathway, Chem. Biol. Drug Des. 93 (2019) 617–627.

[33] Y.J. Cui, C. Liu, C.C. Ma, Y.T. Ji, Y.L. Yao, L.Q. Tang, C.M. Zhang, J.D. Wu, Z.P. Liu, SAR Investigation and Discovery of Water-Soluble 1-Methyl-1,4-dihydroindeno [1,2-c]pyrazoles as Potent Tubulin Polymerization Inhibitors, J. Med. Chem. 63 (2020) 14840–14866.